Title: Mesenchymal stem cells enhance NOX2 dependent ROS production and bacterial killing in macrophages during sepsis

Authors: *Razieh Rabani[1], *Allen Volchuk[1], Mirjana Jerkic[1], Lindsay Ormesher[1], Linda Garces-Ramirez[1,2], Johnathan Canton[3], Claire Masterson[1], Stephane Gagnon[1], Kate C Tatham[1,4], John Marshall[1,5], Sergio Grinstein[3], John G Laffey[1,6,7], #Katalin Szaszi[1,5], #Gerard F Curley[1,7,8]
*, # Contributed equally

Affiliations: [1]Critical Illness and Injury Research Centre, Keenan Research Centre for Biomedical Science of St. Michael's Hospital, Toronto, Canada (Work was performed here); [2]Escuela Nacional de Ciencias Biologicas, Physiology Department, Mexico City, Mexico; [3]Cell Biology Program, The Hospital for Sick Children, Toronto, Canada; [4]Section of Anaesthetics, Pain Medicine and Intensive Care, Department of Surgery and Cancer, Imperial College London, United Kingdom; Departments of [5]Surgery, [6]Physiology and [7]Anesthesia, University of Toronto, Canada; [8]Department of Anaesthesia and Critical Care, Royal College of Surgeons in Ireland, Dublin, Ireland

Correspondance: G.F. Curley, Associate Scientist, Keenan Research Centre for Biomedical Science of St Michael's Hospital; Professor of Anaesthesia and Critical Care, Royal College of Surgeons in Ireland Education and Research Centre, Beaumont Hospital, Dublin, D09 YD60. Email gercurley@rcsi.ie; Phone + 353 1 8093810

"Take home message": Mesenchymal stem cells enhance bacterial killing via production of phagosomal reactive oxygen species in macrophages

ABSTRACT

Human Mesenchymal Stem/Stromal Cells (MSCs) have been reported to produce an M2-like, alternatively activated phenotype in macrophages. In addition, MSCs mediate effective bacterial clearance in pre-clinical sepsis models. Thus, MSCs have a paradoxical anti-microbial and anti-inflammatory response that is not understood. Here we studied the phenotypic and functional response of monocyte-derived human macrophages to MSC exposure *in vitro*.

MSCs induced two distinct, co-existent phenotypes: M2-like macrophages (generally elongated morphology, CD163 positive, acute phagosomal acidification, low NADPH oxidase expression and low phagosomal superoxide production) and M1-like macrophages, characterized by high levels of phagosomal superoxide production. Enhanced phagosomal ROS production was also observed in alveolar macrophages from a rodent model of pneumonia-induced sepsis. The production of M1-like macrophages was dependent on PGE2 and PI3 kinase. MSCs enhanced human macrophage phagocytosis of unopsonized bacteria and enhanced bacterial killing compared to untreated macrophages. Bacterial killing was significantly reduced by blockade of NOX2 using diphenyleneiodonium, suggesting that M1-like cells are primarily responsible for this effect. MSCs also enhanced phagocytosis and polarization of M1-like macrophages derived from patients with severe sepsis.

The enhanced anti-microbial capacity (M1-like), and inflammation resolving phenotype (M2-like), may account for the paradoxical effect of these cells in sepsis *in vivo*.

INTRODUCTION

Sepsis is the biggest cause of mortality in critically ill patients [1], and may contribute to one-half of all hospital deaths [2]. Improved treatment of sepsis could offer meaningful improvements in population mortality.

Mesenchymal stem/stromal cells (MSCs) are stromal cells that form a supportive, perivascular niche for hematopoietic stem cells (HSCs) in bone marrow and coordinate the trafficking of HSCs and monocytes [3, 4]. Although initially identified in bone marrow [5], MSCs are also present as perivascular cells in other tissues, including muscle, umbilical cord and adipose tissue [6], and are easily isolated and expanded in culture. MSCs have demonstrated promise in pre-clinical models [7-9] such that they are being tested in early phase clinical trials in critically ill patients with sepsis (NCT02421484) [10].

A key interaction for the therapeutic benefit of MSCs is that of MSCs and monocytes/macrophages. MSCs have been shown to alter the behavior of mononuclear phagocytes to induce an anti-inflammatory (M2) or tolerant phenotype [11]. MSCs facilitate monocyte to macrophage transition, attenuate activated M1 macrophages and enhance M2 activation [12]. This MSC-mediated modulation of monocyte/macrophage immune responses is believed to play a critical role in their therapeutic effects [13]. M2 macrophages suppress inflammation and facilitate wound repair, but have limited cellular machinery capable of effective microbicidal responses, including the powerful oxidative system composed of the NADPH oxidase [14]. In fact, IL-10 secreting M2 macrophages are particularly adept at suppressing antimicrobial immunity and can enhance the survival and spread of some microorganisms [15, 16]. However, this anti-inflammatory phenotype is inconsistent with several studies, which have demonstrated MSCs to be effective in improving bacterial clearance and survival in animal models of sepsis, an effect that appears dependent in part on macrophages [13, 17-19].

Thus, it remains unclear how MSCs can enhance both bacterial clearance and induce an anti-inflammatory macrophage phenotype.

To better define the effect of MSCs on macrophages, we studied human macrophage phenotype and function in response to human bone marrow-derived MSC exposure. Specifically, we wished to define how exposure to MSCs alter macrophage polarization and key functions such as superoxide production and phagocytosis. Finally, we also aimed at identifying some of the mediators and signaling pathways through which MSCs alter macrophage functions.

MATERIALS AND METHODS

All work was approved by the Human Ethics Committee and the Animal Care and Use Committee of the Keenan Research Centre for Biomedical Science of St Michael's Hospital, Toronto and conducted under license from Health Canada. Detailed methods are described in the Online Data Supplement.

MSC, fibroblasts and monocyte/macrophage isolation and culture

Human bone marrow MSCs were obtained from the Center for the Preparation and Distribution of Adult Stem Cells (medicine.tamhsc.edu/irm/msc-distribution.html) at Texas A&M Health Science Center College of Medicine Institute for Regenerative Medicine (Temple, USA). Human umbilical cord MSCs were provided by Tissue Regeneration Therapeutics (TRT) Inc., Toronto, Canada. The cells fulfilled international criteria. Human normal dermal fibroblasts were purchased from Lonza, Canada. Human peripheral blood mononuclear cells (PBMCs) were isolated from the blood of healthy adult donors or patients with sepsis using dextran/Ficoll or Lympholyte H cell separation media (Cedarlane Cat#CL5015). Detailed protocols are provided in the Online Data Supplement. Briefly, following isolation human blood-derived monocytes were cultured for 8 days with media containing serum (defined as M0 macrophages) or after 5 days the cells were cultured with bone barrow-derived MSCs in transwell (TW) or co-culture for 3 days as indicated in the figure legends. For production of defined M1 or M2 macrophages, monocytes were treated with M-CSF(25 ng/ml) for 6 days then IL-4 (10 ng/ml) for 2 days (M2), or GM-CSF (25 ng/ml) for 6 days then IFNg (10 ng/ml) and LPS (500 ng/ml) for 2 days (M1), as reported previously [14].

Serum-opsonized zymosan and nitroblue tetrazolium (NBT) assay

Dried Zymosan A (*S. cerevisiae*) Bioparticles (Life Technologies) were labeled with fluorophores (Alexa-555 or FITC) as reported previously [14]. NBT assays were performed as described previously [14]. Briefly, Alexa-555-conjugated SOZ and nitroblue tetrazolium (NBT, Sigma Cat#N5514-25TAB) were added to cells at the concentrations indicated in the figure legends for 30 minutes, washed and then fixed in 4% paraformaldehyde in PBS for 15 minutes. Cells were visualized by differential interference contrast microscopy. Dark formazan deposits were indicative of phagosomal superoxide production. In some experiments after the NBT assay the cells were fixed in ice-cold methanol for 2 min at -20 ˚C and processed for immunofluorescence microscopy.

Bacterial phagocytosis, phagosomal pH measurements and killing assay

Cultures of Red Fluorescent Protein (RFP)-expressing *E. coli (DH5a)* or RFP expressing *Burkholderia cenocepacia* were added to macrophage cells at the concentration indicated in the figure legends, washed and fixed in 4% PFA/BSA for 15 minutes. Bacterial phagocytosis was monitored by spinning disk confocal microscopy. Phagosomal pH was measured using ratio imaging as described previously [14]. For bacterial killing, the gentamicin exclusion assay was used, as described in the Online Data Supplement.

Rodent *E. coli* induced Injury

Specific-pathogen-free adult male Sprague Dawley rats (Charles River Laboratories, Quebec, Canada) weighing between 350–450g were used in all experiments. Animals were anesthetized and intubated with a size 14G intravenous catheter (BD Insyte®, Becton Dickinson Ltd, Oxford, UK). 2×10^9 CFU of *E. coli* in a 300 μl PBS suspension was instilled into the trachea using a 1 ml syringe, and the animals allowed to recover and treated with 10×10^6 MSCs/kg or PBS [20]. After 48 hours animals were killed by exsanguination under anesthesia. The heart-lung block was dissected from the thorax,

bronchoalveolar lavage (BAL) was performed, and alveolar macrophages were isolated using Lympholyte R cell separation media (Cedarlane Cat#CL5041).

Statistical Analysis

All values reported are mean ±SD or ±SE as stated in the figure legends. An unpaired t-test assuming equal variance was used for two condition comparisons. ANOVA followed by Tukey's post-hoc test was used for multiple condition comparison. $p<0.05$ was considered significant.

RESULTS

MSCs promote production of phagosomal ROS in macrophages *in vitro* and *in vivo*

MSCs have been reported to enhance bacterial clearance in several animal models of infection *in vivo*, although the precise mechanism remains unclear [13, 17-19, 21]. Mitochondrial transfer [21, 22], production of antimicrobial peptides LL-37 [23], and lipocalin 2 [24] have been shown to be involved in bacterial clearance by MSCs. Moreover, M1 macrophages in particular are thought to have potent anti-microbial capacity in part due to high levels and activity of the phagosomal NADPH oxidase that facilitates bacterial killing [14]. To examine the effect of MSCs on macrophage phagosomal oxidase activity human bone marrow-derived MSCs were co-cultured with human monocyte-derived macrophages and phagosomal superoxide was monitored by exposing macrophages to serum opsonized zymozan (SOZ) in the presence of nitroblue tetrazolium (NBT). The product of NBT reacting with superoxide is formazan, a dark deposit easily visualized by light microscopy [14].

Remarkably, as shown in **Fig. 1A,B,** under conditions where limited or no phagosomal superoxide was detected in control M0 cells (white arrows), many formazan positive cells were apparent in M0 cells that were exposed to MSCs (**Fig. 1A**, yellow arrows). This M1-like phenotype was observed in both transwell and co-culture conditions. M0 cells exposed to fibroblasts rather than MSCs demonstrated no change in production of superoxide

(**Supplemental Fig. 1**). Formazan production was dependent on NADPH oxidase activity since no cells with phagosomal formazan deposits were observed in M0+MSC cells treated with the NADPH oxidase inhibitor diphenyleneiodonium (DPI) **(Fig. 1A)**, which did not affect the ability of the cells to phagocytose SOZ. Overall, under the conditions of the experiment, there was an ~3-fold increase in formazan positive macrophages exposed to MSCs in transwell compared to M0 control (**Fig. 1B**). Additionally, we observed that at high NBT concentrations, where now most of the round cells produced phagosomal formazan (**Fig. 1C**, yellow arrows), a subset of mostly elongated macrophages in the M0+MSC condition were completely devoid of phagosomal formazan (**Fig. 1C**, inset, white arrows). This is indicative of very limited phagosomal superoxide production, which is a feature of M2 macrophages [14] (**Fig. 1C**, right panel). To verify that macrophage phagosomal oxidase activity is indeed enhanced by MSC exposure we performed a luminol assay in live macrophages **(Fig 2A and B)**. Analysis of multiple experiments revealed a significant increase in phagosomal ROS production at early time points in macrophage cells exposed to MSCs (**Fig. 2B**).

In order to determine whether enhanced phagosomal superoxide production in response to MSCs occurs *in vivo*, we isolated macrophages from a rodent model of *E. coli* pneumonia induced sepsis. Alveolar macrophages were isolated after treatment of rats with MSCs or PBS and an NBT assay was performed after isolation and culture. The number of formazan positive cells (indicative of high phagosomal superoxide production) was significantly increased in the MSC-treated condition (**Fig. 3**).

MSC-induced phagosomal ROS production in macrophages is dependent on activation of NADPH-oxidase 2

Given that phagosomal superoxide production is dependent on the NADPH oxidase enzyme, we examined the expression and localization of gp91 (NOX2), the membrane bound catalytic subunit, which has been shown to be expressed at higher levels in M1 compared to M2 macrophages [14]. gp91 expression was readily detected in both control M0 cells, as well as in

macrophage cells in the M0+MSC condition (**Supplemental Fig. 2**) (white arrows). In contrast, elongated M2-like cells observed only in the M0+MSC condition had low gp91 expression (**Supplemental Fig. 2** yellow arrows). gp91 staining in macrophage cells following SOZ phagocytosis in the NBT assay revealed that expression is highest in cells that produce phagosomal superoxide as detected by formazan production (**Supplemental Fig. 2,** white arrowheads), while M2-like cells had lower levels of gp91. However, total gp91 levels in round macrophage cells in the M0+MSC condition were not significantly different from control M0 cells (**Supplemental Fig. 2D and E)**.

Thus, enhanced phagocytosis-induced NADPH oxidase activation, rather than increased levels of the catalytic NOX2 (gp91) subunit, is the more likely mechanism for MSC-induced ROS production in macrophages. Phagocytosis-induced activation of the oxidase is a complex and highly regulated process that involves assembly of a functional multisubunit enzyme complex at the newly forming phagosome by recruitment of several cytosolic subunits to the membrane-bound components gp91^{phox} and p22^{phox} [25, 26]. We examined the localization of one of the cytosolic subunits, p47^{phox}. An NBT assay was performed in M0 cells or M0 exposed to MSCs, followed by immunostaining for p47^{phox}. As shown in **Fig. 4** most M0 cells that phagocytosed SOZ did not produce formazan under the assay conditions used, while most of the p47^{phox} was cytosolic or sequestered in a perinuclear location. In M0 cells exposed to MSCs, phagosomal ROS production was evident as revealed by dark phagosomal formazan deposits (**Fig. 4**, right panels yellow arrows). In these cells many of the zymozan particles were surrounded by bright p47^{phox} immunostaining (**Fig. 4**, left panels yellow arrows). Thus, cells with enhanced ability to produce phagosomal superoxide, which are more prevalent in the M0+MSC condition, have overall increased levels of active oxidase.

MSC-induced phagosomal ROS production is dependent on PGE2 and PI3 kinase

Next, we wished to gain insight into the mechanisms whereby MSC augment oxidase activity. In response to phagocytosis, the cytosolic subunits p47^{phox} and p40^{phox} are recruited to the phagosome by binding to PI (3,4) P2 and PI

(3)P respectively, which are generated by distinct PI3 kinases [25-27]. Thus, we hypothesized that PI3 kinase activity might be increased in some M0 cells exposed to MSCs and that this may in part contribute to the enhanced ability to recruit the cytosolic oxidase subunits, resulting in enhanced ability to activate the oxidase in response to a phagocytic stimulus. Analysis of phospho-Akt, a down-stream target of the PI3 kinase pathway, showed an increase in M0 cells exposed to MSCs compared to M0 alone (**Fig. 5A**). Furthermore, inhibition of PI3 kinase activity with wortmannin prevented the increase in cells with enhanced phagosomal superoxide production (**Fig. 5B**) without affecting SOZ phagocytosis (**Fig. 5C**), indicating that PI3 kinase activity is required for this effect. Similar results were obtained with the PI3 kinase inhibitor LY294002 (results not shown).

PI 3 kinase can be activated by a number of factors including PGE2, which is known to be produced by MSCs [13]. Indeed, PGE2 alone enhances phospho-Akt levels in human M0 macrophages (**Fig. 5D**) and PGE2 levels are markedly enhanced when MSCs are co-cultured with macrophages (**Fig. 5E**). To test whether PGE2 is required for the increase in the number of cells with enhanced phagosomal ROS, we inhibited PGE2 production with CAY10526, which prevented the increase in ROS positive macrophages in response to MSC exposure (**Fig. 5F**). Thus, MSC production of PGE2 could lead to enhanced PI3 kinase activation in a subset of macrophages and allow for enhanced (NOX2) NADPH oxidase assembly in response to phagocytosis resulting in enhanced phagosomal ROS production.

MSCs promote some features of M2-like macrophages

Previous studies have identified that MSCs polarize a population of macrophages resembling an M2-like phenotype [28]. Our results support and extend these findings. Analysis of cell morphology revealed that some macrophage cells cultured with MSCs in transwell had an elongated appearance that is typical of many M2 cells (**Fig. 6A**). Quantification revealed that MSCs caused ~20% of the population to adopt this morphology (**Fig. 6B**). An important functional characteristic of M2 cells is that, in contrast to M1 cells, they rapidly acidify newly formed phagosomes [14]. To determine if the

MSC-induced M2-“like”-cells behaved like bona-fide M2 cells, we monitored phagosomal pH by ratio imaging in macrophage cells exposed to FITC-labelled serum opsonized zymozan (SOZ). Elongated macrophage cells produced in response to MSC exposure rapidly acidified newly formed phagosomes as observed by the drop in the 490nm/444nm excitation wavelength ratio (**Fig. 6C**), similar to M2 cells [14].

M2 macrophages are also distinguished by the expression of certain cell surface proteins [29, 30], such as CD163 in human cells [30, 31]. We monitored localization and levels of CD163 by immunofluorescence microscopy using a specific antibody [32]. The number of cells with CD163 immunostaining (both round and elongated) was higher in M0 cells exposed to MSCs compared to control M0 cells (**Fig. 6D**). Quantification of total fluorescence (**Fig. 6E**) and surface levels by flow cytometry (**Fig. 6F**) showed that MSC-treated macrophages express CD163 at levels higher than M0 cells or defined M2 cells.

Given that phagosomal ROS production is a feature of M1 macrophages, we determined whether M0 cells exposed to MSCs, particularly those with enhanced ROS production, had enhanced levels of M1-specific proteins such as CD40 [29]. Immunofluorescence microscopy confirmed CD40 surface staining in M1 macrophages that produce phagosomal superoxide as detected by the NBT assay (**Supplemental Fig. 3)**. However, macrophages exposed to MSCs had little or no CD40 staining (**Supplemental Fig. 3**). Thus, although M1-like cells have some features of M1 cells, such as high phagosomal superoxide production, they lack markers of bona-fide inflammatory M1 cells.

MSCs enhance bacterial phagocytosis and killing in healthy human macrophages and in macrophages from patients with sepsis

Given that the NADPH oxidase has an essential role in microbicidal capacity [26] and we observe an increase in cells with enhanced oxidase activity, we hypothesized that MSCs may promote bacterial killing via this mechanism. Phagocytosis of unopsonized *Escherichia coli* (**Fig. 7A-C**) and *Burkholderia*

cenocepacia (**Supplemental Fig. 4**) was markedly increased in macrophage cells that had been exposed to MSCs either in transwell or co-culture. We next examined the effect of MSCs on bacterial killing. As shown in **Fig. 7D** macrophage cells that had been exposed to MSCs had greater capacity to kill *E. coli* compared to control M0 or M2 cells. Bacterial killing was markedly reduced by inhibition of the NADPH oxidase with DPI, suggesting that M1-like cells are likely primarily responsible for the enhanced bacterial killing observed.

Given the pre-clinical evidence for MSCs as a novel adjunct to antibiotic therapy, we also examined the effect of MSCs on monocyte-derived macrophages isolated from patients with sepsis. MSCs enhanced phagocytosis of SOZ and production of phagosomal ROS **(Fig. 8A and B)**, as well as phagocytosis of *E. coli* **(Fig. 8C and D)**. This suggests that MSCs could enhance macrophage phagocytosis and bacterial killing in sepsis.

DISCUSSION

In this study we have uncovered the ability of bone marrow-derived MSCs to affect macrophage polarization and function, *in vitro* and *in vivo,* to induce a heterogenous population. Our studies implicate PGE_2 as an important mediator of the effect (Figure 9). To our knowledge we are the first to report such a striking heterogeneity in monocyte-derived macrophages exposed to MSCs. Unexpectedly, we found that MSCs induce co-existent M1-like and M2-like macrophage phenotypes. The fact that macrophages can be directed to a phenotype endowed with enhanced anti-microbial capacity (M1-like), and also an inflammation resolving and tissue repair phenotype (M2-like), may account for the paradoxical effect of these cells in pathogenic conditions such as sepsis *in vivo*.

Previous work in this area by Kim and Hematti [28] and others [13, 33, 34] have described a population of M2-like human macrophages generated *in vitro* after co-culture with human MSCs, defined as CD206-positive, IL-10–high, IL-12–low, IL-6–high, and TNF-α–low. Here, we find that the M2-like macrophage phenotype induced by MSCs in a fraction of the population

indeed had many features associated with M2 macrophage cells, including elongated shape [35], surface markers (CD163), acute phagosomal acidification and low NOX2 expression with limited phagosomal superoxide production [14].

Remarkably, MSCs also induced an M1-like macrophage phenotype in a portion of the macrophage population, characterized by enhanced phagosomal superoxide production. However, unlike defined M1 macrophages, MSC-induced M1-like cells have low or undetectable levels of the M1 macrophage marker CD40. Importantly, this M1-like phenotype was also observed in isolated alveolar macrophages from an *in vivo* rodent model of *E. coli* pneumonia in response to intravenous MSC treatment.

We found that MSCs induced PI3 kinase and PGE2 dependent increase in NOX activity. We also demonstrated an enhanced ability to kill *E. coli* in macrophages exposed to MSCs, which was significantly impaired by inhibition of the NADPH oxidase. It is well established that activation of the phagocyte NADPH oxidase (NOX2) is a vital innate immune mechanism [26]. Indeed, many intra-cellular pathogens are known to thrive in the acidic phagolysosome, such as *Leishmania* spp., are particularly sensitive to ROS-mediated killing [36, 37]. The NADPH oxidase catalyzes the formation of the highly unstable superoxide anion, which can be converted to hydrogen peroxide. Both of these ROS can damage proteins, lipids and DNA resulting in microbicidal activity [38]. Our data support a key role for augmented NADPH oxidase (NOX2) induced by MSCs plays a key role in MSC-induced enhanced bacterial killing. MSCs also enhance phagocytosis and phagosomal ROS generation in macrophages obtained from patients with severe sepsis. Monocyte anergy and immune suppression contributes to an increased risk of adverse events in sepsis [39]. Restoration of monocyte/macrophage antimicrobial function with MSCs represents a promising therapeutic strategy. Our findings provide strong support that MSCs can indeed promote such an improved microbial clearance. We suggest that augmented phagocytosis and oxidase-mediated killing could be one of the mechanisms for the beneficial therapeutic effects of MSCs.

Reactive oxygen species play a critical role in a multitude of cellular processes, including destruction of phagocytosed bacteria [40]. Given the novel M1-like phenotype uncovered, we focused our efforts on identifying how MSCs might mediate enhanced phagosomal ROS production in macrophages. The phagocytic NADPH oxidase complex (NOX2), which consists of membrane-bound subunits (gp91^{phox} and p22^{phox}) and an array of cytoplasmic factors (p40^{phox}, p47^{phox}, p67^{phox}, and Rac) that translocate to the membrane resulting in formation of a primed and active NOX2 complex. We found that oxidase assembly is increased in macrophages with enhanced ability to produce phagosomal superoxide, as monitored by the distribution of p47^{phox} in the NBT assay and that PI 3-kinase activity is essential for the increase in M1-like cells. Basal PI 3-kinase activity was enhanced in the macrophage population exposed to MSCs. Presumably this would enhance the ability to recruit cytosolic oxidase components in a subset of macrophages in response to phagocytosis, which is dependent on the production of phosphoinositides to facilitate the recruitment of cytosolic oxidase subunits to the membrane bound subunits at the forming phagosome [25-27].

NOX2 activation by MSCs in our study is PGE2 dependent. However, prostanoids, including PGE_2, have traditionally been believed to exert anti-inflammatory effects in macrophages. PGE_2 has been demonstrated to inhibit the production of pro-inflammatory molecules such as TNF-α [41] and increase the secretion of anti-inflammatory cytokines, such as IL-10 [42]. Regarding the MSC-mediated polarization of macrophages to an M2 phenotype, a major role has been ascribed to prostaglandin E_2 [13]. However, studies of prostanoid receptors in mice, on helper T (T_H)-cells and dendritic cells revealed that different prostanoid receptors regulate the immune response at various steps by exerting often opposing actions [43, 44]. In particular, although PGE_2 suppresses pro-inflammatory actions of macrophages and T_H1 differentiation by raising intracellular cyclic AMP (cAMP) concentrations, PGE_2 also facilitates T_H1 differentiation via P13K. Moreover, PGE2 induces production of ROS in mast cells in a PI3K-dependent manner [45]. Here, we demonstrated that inhibition of MSC-

derived PGE_2 prevented MSC-induced phagosomal ROS production, while co-culture of MSCs and macrophages induces enhanced production of PGE_2 from MSCs. PGE_2 alone activated PI 3-kinase and ROS production in macrophages. Diverse functions of PGE2 may be dependent on several factors including differential expression of EP receptors on macrophages [46], dynamics of EP receptors expression during the course of macrophage activation [47], differences in ligand affinity of EP receptors and kinetics of the receptors desensitization, and finally the specific downstream pathways of each receptor [48].

It is also important to point out that although the NADPH oxidase is a key component of the anti-bacterial response, other factors may also contribute to enhanced bacterial killing. Indeed, although M2 cells have limited NOX2 expression they were still able to kill *E. coli*, although less efficiently than M1 or M1-like cells. Presumably, this is due to the degradative capacity in the low pH environment of the phagolysosome [49]. Furthermore, mitochondrial ROS has also been implicated in contributing to pathogen killing [50], and recent studies have shown that MSCs can potentially deliver mitochondria to macrophage cells via extracellular vesicles [51] and via tunneling nanotubules [21].

How do MSCs produce different macrophage phenotypes from the same blood-derived monocytes? At least three distinct types of blood-derived monocytes exist [52] and presumably at least one of these populations gives rise to macrophages that respond to PGE_2 to produce the M1-like phenotype we have observed. As we, and others, have shown [11, 13], MSCs also induce an M2-like phenotype from monocytes. This directed maturation is partially regulated via direct cell contact, but also by MSC secretion of PGE2, IL-6, IDO and TSG-6 [13, 33, 34, 53]. However, other factors may also contribute to MSC-induced effects. Other investigators [22, 51] have recently demonstrated that macrophages engulf mitochondria-containing microvesicles and microRNA-containing exosomes from MSCs thereby enhancing macrophage bioenergetics while inhibiting macrophage activation. Lee *et al* have demonstrated some antimicrobial effects of MSC-secreted keratinocyte

growth factor and microvesicles on human monocytes [54, 55]. What is clear from these and our own studies is that MSC immune modulation of monocytes and macrophages is complex, likely not accomplished by a single secreted factor and represents a balance of pro- and anti-inflammatory stimulation.

There are a number of limitations to these experiments. MSCs modulate macrophage function and bacterial killing by a variety of mechanisms unexamined in these studies, including transfer of mitochondria and regulatory microRNAs [51], and secretion of antimicrobial peptides [23]. We focused on PGE2, as it has an important role in MSC effects in sepsis, as well as macrophage polarisation [13]. We did not augment PGE2 secretion in our studies, which could serve as a mechanism to enhance MSC potency, although this approach is likely to have off-target effects. The timing of the effect also needs further evaluation: our *in vitro* experiments involved 48-72 hours exposure of macrophages to MSCs, which may not reflect *in vivo* MSC-macrophage interactions. Although our studies examined effects of MSCs on macrophages from healthy volunteers, as well as septic patients, we did not isolate macrophages from critically ill patients without sepsis. It is likely, however, that MSCs alter phagocytosis and ROS generation in a similar manner to healthy controls. Finally, future studies, using single cell RNA sequencing and bioinformatics approaches, could provide a more detailed characterization of the heterogeneous macrophage populations we have observed.

The future of MSC therapy depends on the development of a potent, consistent cell-based therapeutic. While cell-free approaches, using MSC-derived extracellular vesicles (EVs), have emerged as a promising treatment strategy, we have observed a synergy and crosstalk between MSCs and macrophages, which points to the need for the cell itself to achieve maximal therapeutic effect. Factors limiting the potential of MSCs as a therapy for sepsis include limited MSC persistence, insufficient and variable immunomodulatory potency and dependence on *in vivo* activation by host inflammatory mediators [56]. Detailed understanding of the host response to

MSCs, as in this study and others [21, 51], is necessary in order to develop a consistent therapeutic and to identify patients most likely to benefit. Previous clinical trials of MSCs for other disease indications demonstrate the need to develop *in vitro* and *in vivo* models that can predict successful host response to MSC therapy [57]. Our study identifies phagocytosis and ROS production as host factors during sepsis that could be rescued by MSC treatment.

Acknowledgements

We would like to thank Chris Spring for assistance with flow cytometry analysis and Professor JED Davies and Tissue Regeneration Therapeutics for providing umbilical cord mesenchymal stem cells.

Funding Support: G. Curley and J Laffey are funded by the Canadian Institutes of Health Research (CIHR-312714) and hold a Merit Award and a Clinician Scientist Transition Award respectively, from the University of Toronto, Department of Anesthesia. G. Curley holds an award from the International Anesthesia Research Society and is funded by a Government of Ontario, Ministry of Research and Innovation, Early Researcher Award. G Curley and K Szaszi were funded by an award from St Michael's Hospital Translational Innovation Fund. KC Tatham is funded by the National Institute of Health Research (UK), the European Institute of Innovation and Technology and Academy of Medical Sciences (UK).

Competing interests

The authors have no competing interests to disclose.

REFERENCES

1. Brun-Buisson C, Meshaka P, Pinton P, Vallet B, Group ES. EPISEPSIS: a reappraisal of the epidemiology and outcome of severe sepsis in French intensive care units. *Intensive Care Med* 2004: 30(4): 580-588.
2. Liu V, Escobar GJ, Greene JD, Soule J, Whippy A, Angus DC, Iwashyna TJ. Hospital deaths in patients with sepsis from 2 independent cohorts. *JAMA* 2014: 312(1): 90-92.
3. Mendez-Ferrer S, Michurina TV, Ferraro F, Mazloom AR, Macarthur BD, Lira SA, Scadden DT, Ma'ayan A, Enikolopov GN, Frenette PS. Mesenchymal and haematopoietic stem cells form a unique bone marrow niche. *Nature* 2010: 466(7308): 829-834.
4. Shi C, Jia T, Mendez-Ferrer S, Hohl TM, Serbina NV, Lipuma L, Leiner I, Li MO, Frenette PS, Pamer EG. Bone marrow mesenchymal stem and progenitor cells induce monocyte emigration in response to circulating toll-like receptor ligands. *Immunity* 2011: 34(4): 590-601.
5. Friedenstein AJ, Petrakova KV, Kurolesova AI, Frolova GP. Heterotopic of bone marrow. Analysis of precursor cells for osteogenic and hematopoietic tissues. *Transplantation* 1968: 6(2): 230-247.
6. Crisan M, Yap S, Casteilla L, Chen CW, Corselli M, Park TS, Andriolo G, Sun B, Zheng B, Zhang L, Norotte C, Teng PN, Traas J, Schugar R, Deasy BM, Badylak S, Buhring HJ, Giacobino JP, Lazzari L, Huard J, Peault B. A perivascular origin for mesenchymal stem cells in multiple human organs. *Cell Stem Cell* 2008: 3(3): 301-313.
7. Curley GF, Ansari B, Hayes M, Devaney J, Masterson C, Ryan A, Barry F, O'Brien T, Toole DO, Laffey JG. Effects of intratracheal mesenchymal stromal cell therapy during recovery and resolution after ventilator-induced lung injury. *Anesthesiology* 2013: 118(4): 924-932.
8. Curley GF, Hayes M, Ansari B, Shaw G, Ryan A, Barry F, O'Brien T, O'Toole D, Laffey JG. Mesenchymal stem cells enhance recovery and repair following ventilator-induced lung injury in the rat. *Thorax* 2012: 67(6): 496-501.
9. Curley GF, Jerkic M, Dixon S, Hogan G, Masterson C, O'Toole D, Devaney J, Laffey JG. Cryopreserved, Xeno-Free Human Umbilical Cord Mesenchymal Stromal Cells Reduce Lung Injury Severity and Bacterial Burden in Rodent Escherichia coli-Induced Acute Respiratory Distress Syndrome. *Crit Care Med* 2017: 45(2): e202-e212.
10. Liu KD, Wilson JG, Zhuo H, Caballero L, McMillan ML, Fang X, Cosgrove K, Calfee CS, Lee JW, Kangelaris KN, Gotts JE, Rogers AJ, Levitt JE, Wiener-Kronish JP, Delucchi KL, Leavitt AD, McKenna DH, Thompson BT, Matthay MA. Design and implementation of the START (STem cells for ARDS Treatment) trial, a phase 1/2 trial of human mesenchymal stem/stromal cells for the treatment of moderate-severe acute respiratory distress syndrome. *Ann Intensive Care* 2014: 4: 22.
11. Ko JH, Lee HJ, Jeong HJ, Kim MK, Wee WR, Yoon SO, Choi H, Prockop DJ, Oh JY. Mesenchymal stem/stromal cells precondition lung monocytes/macrophages to produce tolerance against allo- and autoimmunity in the eye. *Proc Natl Acad Sci U S A* 2016: 113(1): 158-163.

12. Vasandan AB, Jahnavi S, Shashank C, Prasad P, Kumar A, Prasanna SJ. Human Mesenchymal stem cells program macrophage plasticity by altering their metabolic status via a PGE2-dependent mechanism. *Sci Rep* 2016: 6: 38308.
13. Nemeth K, Leelahavanichkul A, Yuen PST, Mayer B, Parmelee A, Doi K, Robey PG, Leelahavanichkul K, Koller BH, Brown JM, Hu X, Jelinek I, Star RA, Mezey E. Bone marrow stromal cells attenuate sepsis via prostaglandin E2-dependent reprogramming of host macrophages to increase their interleukin-10 production. *Nat Med* 2009: 15: 42-49.
14. Canton J, Khezri R, Glogauer M, Grinstein S. Contrasting phagosome pH regulation and maturation in human M1 and M2 macrophages. *Mol Biol Cell* 2014: 25: 3330-3341.
15. Miles SA, Conrad SM, Alves RG, Jeronimo SM, Mosser DM. A role for IgG immune complexes during infection with the intracellular pathogen Leishmania. *J Exp Med* 2005: 201(5): 747-754.
16. Muller U, Stenzel W, Kohler G, Werner C, Polte T, Hansen G, Schutze N, Straubinger RK, Blessing M, McKenzie AN, Brombacher F, Alber G. IL-13 induces disease-promoting type 2 cytokines, alternatively activated macrophages and allergic inflammation during pulmonary infection of mice with Cryptococcus neoformans. *J Immunol* 2007: 179(8): 5367-5377.
17. Devaney J, Horie S, Masterson C, Elliman S, Barry F, O'Brien T, Curley GF, O'Toole D, Laffey JG. Human mesenchymal stromal cells decrease the severity of acute lung injury induced by E. coli in the rat. *Thorax* 2015: 70(7): 625-635.
18. Krasnodembskaya A, Samarani G, Song Y, Zhuo H, Su X, Lee JW, Gupta N, Petrini M, Matthay MA. Human mesenchymal stem cells reduce mortality and bacteremia in gram-negative sepsis in mice in part by enhancing the phagocytic activity of blood monocytes. *Am J Physiol Lung Cell Mol Physiol* 2012: 302(10): L1003-1013.
19. Mei SH, Haitsma JJ, Dos Santos CC, Deng Y, Lai PF, Slutsky AS, Liles WC, Stewart DJ. Mesenchymal stem cells reduce inflammation while enhancing bacterial clearance and improving survival in sepsis. *Am J Respir Crit Care Med* 2010: 182(8): 1047-1057.
20. O'Croinin DF, Nichol AD, Hopkins N, Boylan J, O'Brien S, O'Connor C, Laffey JG, McLoughlin P. Sustained hypercapnic acidosis during pulmonary infection increases bacterial load and worsens lung injury. *Crit Care Med* 2008: 36(7): 2128-2135.
21. Jackson MV, Morrison TJ, Doherty DF, McAuley DF, Matthay MA, Kissenpfennig A, O'Kane CM, Krasnodembskaya AD. Mitochondrial Transfer via Tunneling Nanotubes (TNT) is an Important Mechanism by which Mesenchymal Stem Cells Enhance Macrophage Phagocytosis in the in vitro and in vivo Models of ARDS. *Stem Cells* 2016.
22. Morrison TJ, Jackson MV, Cunningham EK, Kissenpfennig A, McAuley DF, O'Kane CM, Krasnodembskaya AD. Mesenchymal Stromal Cells Modulate Macrophages in Clinically Relevant Lung Injury Models by Extracellular Vesicle Mitochondrial Transfer. *Am J Respir Crit Care Med* 2017.
23. Krasnodembskaya A, Song Y, Fang X, Gupta N, Serikov V, Lee JW, Matthay MA. Antibacterial effect of human mesenchymal stem cells is mediated in part from secretion of the antimicrobial peptide LL-37. *Stem Cells* 2010: 28(12): 2229-2238.

24. Gupta N, Krasnodembskaya A, Kapetanaki M, Mouded M, Tan X, Serikov V, Matthay MA. Mesenchymal stem cells enhance survival and bacterial clearance in murine Escherichia coli pneumonia. *Thorax* 2012: 67(6): 533-539.
25. Leto TL, Morand S, Hurt D, Ueyama T. Targeting and regulation of reactive oxygen species generation by Nox family NADPH oxidases. *Antioxid Redox Signal* 2009: 11(10): 2607-2619.
26. Nunes P, Demaurex N, Dinauer MC. Regulation of the NADPH oxidase and associated ion fluxes during phagocytosis. *Traffic* 2013: 14(11): 1118-1131.
27. Vieira OV, Botelho RJ, Rameh L, Brachmann SM, Matsuo T, Davidson HW, Schreiber A, Backer JM, Cantley LC, Grinstein S. Distinct roles of class I and class III phosphatidylinositol 3-kinases in phagosome formation and maturation. *J Cell Biol* 2001: 155(1): 19-25.
28. Kim J, Hematti P. Mesenchymal stem cell-educated macrophages: a novel type of alternatively activated macrophages. *Exp Hematology* 2009: 37: 1445-1453.
29. Murray PJ, Allen JE, Biswas SK, Fisher EA, Gilroy DW, Goerdt S, Gordon S, Hamilton JA, Ivashkiv LB, Lawrence T, Locati M, Mantovani A, Martinez FO, Mege J-L, Mosser DM, Natoli G, Saeij JP, Schultze JL, Shirey KA, Sica A, Suttles J, Udalova I, van Ginderachter JA, Vogel SN, Wynn TA. Macrophage activation and polarization: nomenclature and experimental guidelines. *Immunity* 2014: 41: 14-20.
30. Roszer T. Understanding the Mysterious M2 Macrophage through Activation Markers and Effector Mechanisms. *Mediators Inflamm* 2015: 2015: 816460.
31. Jaguin M, Houlbert N, Fardel O, Lecureur V. Polarization profiles of human M-CSF-generated macrophages and comparison of M1-markers in classically activated macrophages from GM-CSF and M-CSF origin. *Cell Immunol* 2013: 281: 51-61.
32. Fuentes-Duculan J, Suarez-Farinas M, Zaba LC, Nograles KE, Pierson KC, Mitsui H, Pensabene CA, Kzhshkowska J, Krueger JG, Lowes MA. A subpopulation of CD163-positive macrophages is classically activated in psoriasis. *J Invest Derm* 2010: 130: 2412-2422.
33. Melief SM, Schrama E, Brugman MH, Tiemessen MM, Hoogduijn MJ, Fibbe WE, Roelofs H. Multipotent stromal cells induce human regulatory T cells through a novel pathway involving skewing of monocytes toward anti-inflammatory macrophages. *Stem Cells* 2013: 31(9): 1980-1991.
34. Francois M, Romieu-Mourez R, Li M, Galipeau J. Human MSC suppression correlates with cytokine induction of indoleamine 2,3-dioxygenase and bystander M2 macrophage differentiation. *Mol Ther* 2012: 20(1): 187-195.
35. McWhorter FY, Wang T, Nguyen P, Chung T, Liu WF. Modulation of macrophage phenotype by cell shape. *Proc Natl Acad Sci U S A* 2013: 110(43): 17253-17258.
36. Novais FO, Nguyen BT, Beiting DP, Carvalho LP, Glennie ND, Passos S, Carvalho EM, Scott P. Human classical monocytes control the intracellular stage of Leishmania braziliensis by reactive oxygen species. *J Infect Dis* 2014: 209(8): 1288-1296.
37. Novais FO, Santiago RC, Bafica A, Khouri R, Afonso L, Borges VM, Brodskyn C, Barral-Netto M, Barral A, de Oliveira CI. Neutrophils and

macrophages cooperate in host resistance against Leishmania braziliensis infection. *J Immunol* 2009: 183(12): 8088-8098.
38. Lam GY, Huang J, Brumell JH. The many roles of NOX2 NADPH oxidase-derived ROS in immunity. *Semin Immunopathol* 2010: 32(4): 415-430.
39. Delano MJ, Ward PA. Sepsis-induced immune dysfunction: can immune therapies reduce mortality? *J Clin Invest* 2016: 126(1): 23-31.
40. DeLeo FR, Allen LA, Apicella M, Nauseef WM. NADPH oxidase activation and assembly during phagocytosis. *J Immunol* 1999: 163(12): 6732-6740.
41. Ratcliffe MJ, Walding A, Shelton PA, Flaherty A, Dougall IG. Activation of E-prostanoid4 and E-prostanoid2 receptors inhibits TNF-alpha release from human alveolar macrophages. *Eur Respir J* 2007: 29(5): 986-994.
42. Menard G, Turmel V, Bissonnette EY. Serotonin modulates the cytokine network in the lung: involvement of prostaglandin E2. *Clin Exp Immunol* 2007: 150(2): 340-348.
43. Kabashima K, Sakata D, Nagamachi M, Miyachi Y, Inaba K, Narumiya S. Prostaglandin E2-EP4 signaling initiates skin immune responses by promoting migration and maturation of Langerhans cells. *Nat Med* 2003: 9(6): 744-749.
44. Yao C, Sakata D, Esaki Y, Li Y, Matsuoka T, Kuroiwa K, Sugimoto Y, Narumiya S. Prostaglandin E2-EP4 signaling promotes immune inflammation through Th1 cell differentiation and Th17 cell expansion. *Nat Med* 2009: 15(6): 633-640.
45. Kuehn HS, Jung MY, Beaven MA, Metcalfe DD, Gilfillan AM. Prostaglandin E2 activates and utilizes mTORC2 as a central signaling locus for the regulation of mast cell chemotaxis and mediator release. *J Biol Chem* 2011: 286(1): 391-402.
46. Sokolowska M, Chen LY, Liu Y, Martinez-Anton A, Qi HY, Logun C, Alsaaty S, Park YH, Kastner DL, Chae JJ, Shelhamer JH. Prostaglandin E2 Inhibits NLRP3 Inflammasome Activation through EP4 Receptor and Intracellular Cyclic AMP in Human Macrophages. *J Immunol* 2015: 194(11): 5472-5487.
47. Hubbard NE, Lee S, Lim D, Erickson KL. Differential mRNA expression of prostaglandin receptor subtypes in macrophage activation. *Prostaglandins Leukot Essent Fatty Acids* 2001: 65(5-6): 287-294.
48. Kalinski P. Regulation of immune responses by prostaglandin E2. *J Immunol* 2012: 188(1): 21-28.
49. Ip WK, Sokolovska A, Charriere GM, Boyer L, Dejardin S, Cappillino MP, Yantosca LM, Takahashi K, Moore KJ, Lacy-Hulbert A, Stuart LM. Phagocytosis and phagosome acidification are required for pathogen processing and MyD88-dependent responses to Staphylococcus aureus. *J Immunol* 2010: 184(12): 7071-7081.
50. West AP, Brodsky IE, Rahner C, Woo DK, Erdjument-Bromage H, Tempst P, Walsh MC, Choi Y, Shadel GS, Ghosh S. TLR signaling augments macrophage bactericidal activity through mitochondrial ROS. *Nature* 2011: 472: 476-480.
51. Phinney DG, Di Giuseppe M, Njah J, Sala E, Shiva S, St Croix CM, Stolz DB, Watkins SC, Di YP, Leikauf GD, Kolls J, Riches DW, Deiuliis G, Kaminski N, Boregowda SV, McKenna DH, Ortiz LA. Mesenchymal stem cells use extracellular vesicles to outsource mitophagy and shuttle microRNAs. *Nat Commun* 2015: 6: 8472.
52. Murray PJ, Wynn TA. Protective and pathogenic functions of macrophage subsets. *Nat Rev Immunol* 2011: 11(11): 723-737.

53. Mittal M, Tiruppathi C, Nepal S, Zhao YY, Grzych D, Soni D, Prockop DJ, Malik AB. TNFalpha-stimulated gene-6 (TSG6) activates macrophage phenotype transition to prevent inflammatory lung injury. *Proc Natl Acad Sci U S A* 2016: 113(50): E8151-E8158.
54. Lee JW, Krasnodembskaya A, McKenna DH, Song Y, Abbott J, Matthay MA. Therapeutic effects of human mesenchymal stem cells in ex vivo human lungs injured with live bacteria. *Am J Respir Crit Care Med* 2013: 187(7): 751-760.
55. Monsel A, Zhu YG, Gennai S, Hao Q, Hu S, Rouby JJ, Rosenzwajg M, Matthay MA, Lee JW. Therapeutic Effects of Human Mesenchymal Stem Cell-derived Microvesicles in Severe Pneumonia in Mice. *Am J Respir Crit Care Med* 2015: 192(3): 324-336.
56. Galipeau J. The mesenchymal stromal cells dilemma--does a negative phase III trial of random donor mesenchymal stromal cells in steroid-resistant graft-versus-host disease represent a death knell or a bump in the road? *Cytotherapy* 2013: 15(1): 2-8.
57. Trounson A, McDonald C. Stem Cell Therapies in Clinical Trials: Progress and Challenges. *Cell Stem Cell* 2015: 17(1): 11-22.

FIGURE LEGENDS

Figure 1. Effect of human MSCs on phagosomal ROS production in human macrophages (NBT assay)

(**A**) Human blood-derived monocytes were cultured for 8 days with media containing serum (M0) or after 5 days the cells were cultured with bone barrow-derived MSCs in transwell (TW) or co-culture for 3 days. The cells were then incubated with 0.01 mg/ml serum-opsonized zymozan (SOZ) together with 0.125 mg/ml nitroblue tetrazolium (NBT) in the absence or presence of 10 μM diphenyleneiodonium (DPI), as indicated. The cells were fixed and imaged by differential interference contrast microscopy. White arrows indicate cells that have phagocytosed SOZ that are devoid of formazan deposits. With MSC exposure numerous cells had clear evidence of phagosomal formazan, indicative of high phagosomal superoxide production (yellow arrows). Representative images shown for the various conditions. (**B**) The percentage of formazan positive cells was quantified (Mean ±SD, n=4 independent experiments: M0, M0+MSC (TW), M2; n=3, M1. (*$p<0.01$, M0 vs. M0+MSC (TW); t-test). (**C**) M0 cells exposed to MSCs (TW) or M2 cells were incubated with SOZ and 2 mg/ml NBT for 30 min. The cells were then washed, fixed and imaged by DIC microscopy. Two phenotypes were observed; most round cells that phagocytosed SOZ had dark formazan deposits (yellow arrows), while elongated cells that phagocytosed SOZ had limited or no formazan deposits in phagosomes (white arrows in inset), similar to M2 cells (right panel).

Figure 2. Effect of human MSCs on phagosomal ROS production in human macrophages (Luminol assay)

Human blood-derived monocytes were seeded in a 96 well plate, cultured for 8 days with media containing serum (M0) or after 5 days the cells were co-cultured with bone barrow-derived MSCs for 3 days. A luminol assay was performed to monitor phagosomal ROS production as described in the Methods. Luminescence in RLU was monitored over time. **A.** Representative

single experiment showing control macrophages not exposed to serum opsonized zymozan (SOZ), or control or MSC-exposed macrophages treated with SOZ. An increase in luminescence is only observed in macrophages that have been exposed to SOZ. **B.** Data normalized to RLU value at t=4 min (n=5 independent experiments, * $p<0.05$).

Figure. 3. Effect of human MSCs on phagosomal ROS production in isolated rat alveolar macrophages from an *E. coli* pneumonia model

Alveolar macrophages were isolated from rats exposed to *E. coli* pneumonia, then either treated with PBS or MSCs for 48h as described in the Methods. An SOZ-NBT assay was then performed. (**A**) Representative images are shown. Phagosomal formazan deposits indicative of phagosomal ROS appear black. (**B**) Quantitation of formazan positive cells from n=4 experiments (Mean ±SD, *$p<0.05$, t-test).

Figure 4. M1-like macrophages have increased phagosomal levels of the NADPH oxidase subunit p47^{phox}

Human macrophages were exposed or not to bone barrow-derived MSCs in transwell (TW) for 3 days. The cells were then incubated with serum-opsonized zymozan (SOZ) together with 0.125 mg/ml NBT for 30 min. The cells were fixed and immunostained for p47^{phox}. In control M0 cells with no detectable phagosomal superoxide production p47^{phox} immunostaining was apparent in a clustered perinuclear region, in the cytosol and weak staining was observed in some cells surrounding internalized zymozan particles (white arrow). In M0 exposed to MSCs (M0+MSC) many cells producing abundant phagosomal superoxide, as detected by dark formazan deposits, were evident (yellow arrows, bottom right panel). In general these cells had higher levels of p47^{phox} immunostaining surrounding internalized zymozan particles (yellow arrows, bottom left panel). Size bar; 10 μm.

Figure. 5. MSC-induced production of M1-like macrophages requires PGE2 and PI 3-kinase

Human blood-derived monocytes were cultured for 8 days with media containing serum (M0) or after 5 days the cells were cultured with bone barrow-derived MSCs in transwell (TW) for 3 days. To monitor PI3K activation in the macrophages exposed to MSCs, total cell lysates were subjected to Western blotting **(A)** with anti-phospho S(473)-Akt. To normalize for protein loading, membrane was probed with anti-total Akt (n=3, mean ±SD; **p<0.01). To confirm the role of PI3K activation, M0 cells were cultured with MSCs in transwell in the absence or presence of 1 μM wortmannin PI3K inhibitor. Then cells were incubated with 0.01 mg/ml serum-opsonized zymozan (SOZ) together with 0.125 mg/ml nitroblue tetrazolium (NBT) for 30 min. The cells then were washed and fixed. the percentage of the formazan positive cells **(B)** and also the percentage of cells phagocytosed SOZ **(C)** were analyzed using disk spinning confocal microscope (n=3, mean ±SD, * M0 vs M0+MSC, p<0.05, ## ctl vs Wortmannin, p<0.01, *** M0 vs M0+MSC, p<0.001). **(D).** Human blood-derived monocytes were cultured for 5 days, followed with stimulation with vehicle or 100nM PGE2 for 24h. Levels of phospho S(473)-Akt and total Akt were analyzed by Western blotting (n=3, mean ±SD; *p<0.05). **(E)**. Levels of PGE2 in culture supernatant of M0, MSC and M0 exposed to MSCs in transwell were analyzed by PGE2 ELISA kit (n=3, mean ±SD; *p<0.05). **(F)**. Human blood-derived monocytes were cultured for 5 days, then co-cultured with MSCs in transwell (TW) for 3 days in the absence or presence of 10 μM PGE2 synthase inhibitor CAY10526. NBT assay was performed as described above and the percentage of formazan positive cells was quantified (n=3, mean ±SD, ** M0 vs M0+MSC, ## ctl vs CAY10526, P<0.01).

Figure 6. MSCs cause some human macrophages to adopt an M2-like morphology and phenotype

(**A**) Human blood-derived monocytes were cultured for 8 days with media containing serum (M0) or after 5 days the cells were cultured with bone barrow-derived MSCs in transwell (TW) for 3 days. M2 cells were generated as described in the methods. The cells were fixed and observed by differential interference contrast microscopy. Many M2 cells adopt an elongated morphology, which were evident in the MO+MSC condition (white arrows), but

not in the M0 condition. (**B**) The % of elongated cells was quantified. Data is mean ±SD from n=7 experiments. (**C**) Human blood-derived monocytes were cultured for 5 days then cultured with MSCs for 3 days (TW). Phagosomal pH was monitored in M2-like cells by ratio imaging using FITC-SOZ as outlined in the methods. In some experiments external non-phagocytosed FITC-SOZ particles were also imaged as a control. Data shown is from n=3-4 independent experiments (mean 490nm /440nm ratio ±SD). (**D**) Macrophages were prepared as described in (A) then fixed and immunostained for CD163. Representative confocal images (25X magnification. Size bar; 20 μm). (**E**) Cellular fluorescence intensity was measured using ImageJ and values were normalized to the levels in M0 cells (Mean ±SD from n=3 experiments) (*p<0.01, M2 vs M0+MSC). (**F**) Flow cytometry analysis of CD163 in the various conditions. Mean fluorescence intensity (MFI) of the positive cell population (n=4, *p<0.05, M2 vs M0+MSC).

Figure 7. MSC exposure enhances *E. coli* phagocytosis and killing

(**A**) Human blood-derived monocytes were cultured for 8 days with media containing serum (M0) or after 5 days the cells were cultured with bone barrow-derived MSCs in transwell (TW) or co-culture for 3 days. The cells were then incubated with live RFP-expressing *E. coli* which were spun down onto the macrophage cells. After 20 min the cells were washed with PBS, fixed, then imaged by light and fluorescence microscopy. Representative extended focus images of combined phase contrast and RFP fluorescence. Size bar; 10 μm. (**B**) The % of cells that phagocytosed bacteria (n=4-5 independents experiments, mean ±SE; *p<0.01). (**C**) The number of *E. coli* cells phagocytosed or bound per macrophage cell was quantified (n=4-5 independent experiments, mean ±SE). p<0.05, M0 vs M0+MSC (TW or co-culture); ANOVA and Tukey's test. (**D**) Macrophage cells were prepared as described in (A) and assessment of phagocytic *E. coli* killing was performed as outlined in the Methods. n=6 independent experiments (M0, M0+MSC, M2); n=4 (MO+MSC; +10 μM DPI); n=3 (M1). ANOVA followed by Tukey's post-hoc test was to assess statistical significance.

Figure 8. MSCs induce M1-like and M2-like phenotypes and enhance phagocytosis in macrophages derived from patients with sepsis

(**A**) Human blood-derived monocytes were isolated from patients with sepsis and cultured for 8 days with media containing serum (M0) or after 5 days the cells were cultured with bone barrow-derived MSCs in transwell (TW) for 3 days. An SOZ-NBT assay was performed as in Fig. 1A. The cells were fixed and imaged by confocal microscopy. Both M2-like cells (white arrows) and M1-like cells with detectable phagosomal formazan (yellow arrows) were observed. Result is representative of n=4 patients. Images are 25X mag. Size bar; 20 μm. (**B**) Quantification of phagosomal formazan positive cells (n=4, Mean ±SD; *p<0.05). (**C**) Cells were prepared as in (A) and *E. coli* phagocytosis was monitored as described in the Methods. MSC exposed macrophages had increased levels of intracellular or bound *E. coli*. Representative images. Size bar; 10 μm. (**D**) The number of *E. coli* cells phagocytosed or bound per macrophage cell was quantified (n=3 patients, mean ±SD, *p<0.05).

Figure 9. Schematic showing the mechanisms by which MSCs alter macrophages function

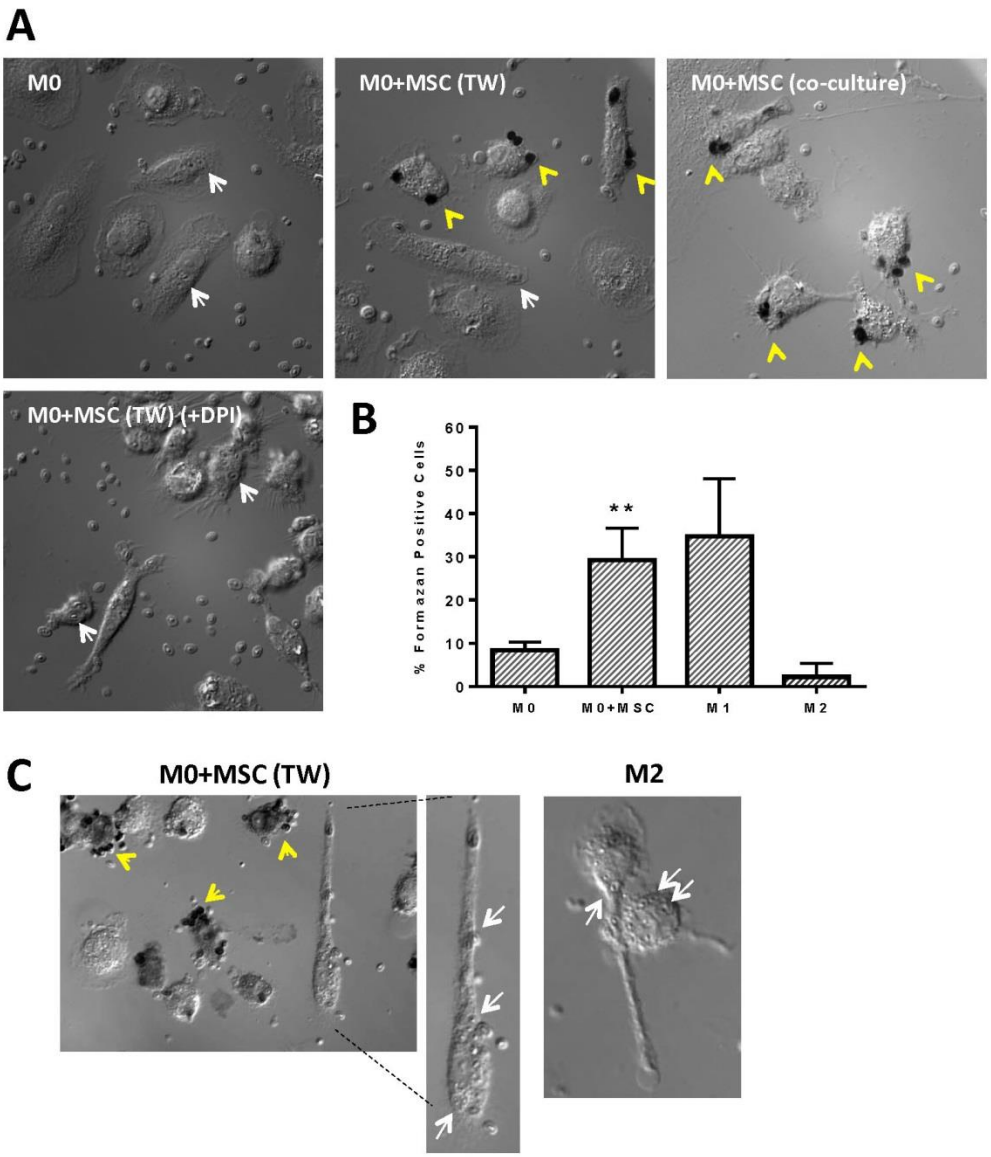
A
M0
M0+MSC (TW)
M0+MSC (co-culture)
M0+MSC (TW) (+DPI)
B
% Formazan Positive Cells
60
50
40
30
20
10
0
**
M0
M0+MSC
M1
M2
C
M0+MSC (TW)
M2

Figure 1

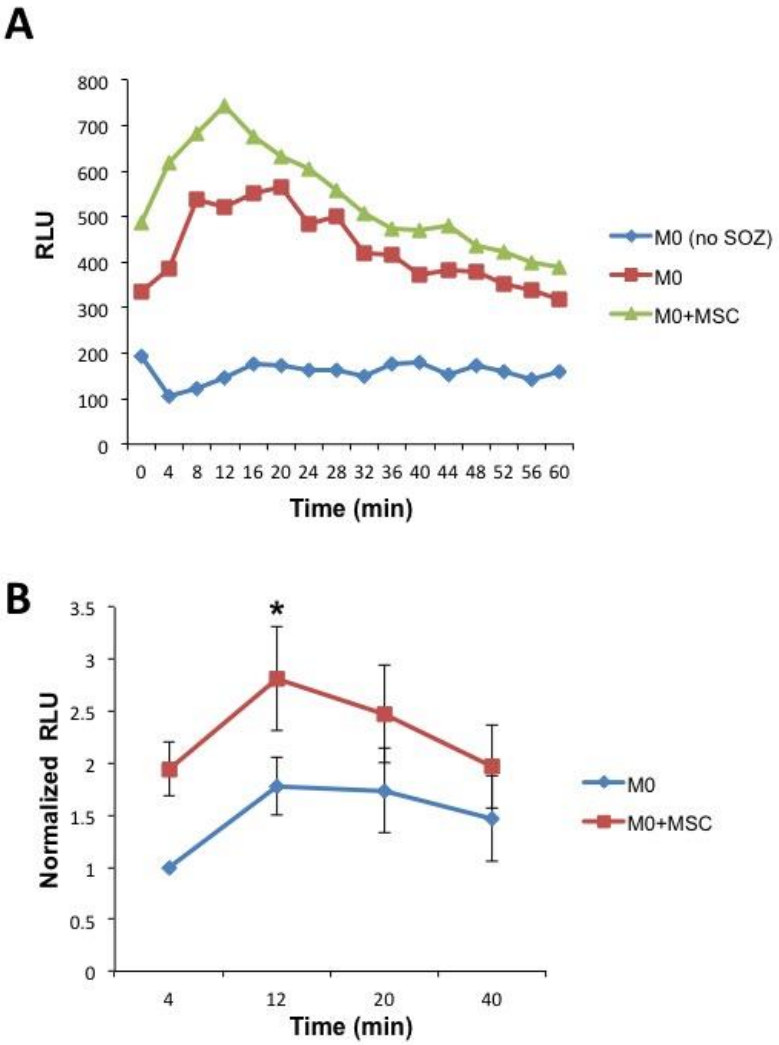
A
800
700
600
500
400
300
200
100
0
RLU
0 4 8 12 16 20 24 28 32 36 40 44 48 52 56 60
Time (min)
M0 (no SOZ)
M0
M0+MSC
B
3.5
3
2.5
2
1.5
1
0.5
0
Normalized RLU
*
4
12
20
40
Time (min)
M0
M0+MSC

Figure 2

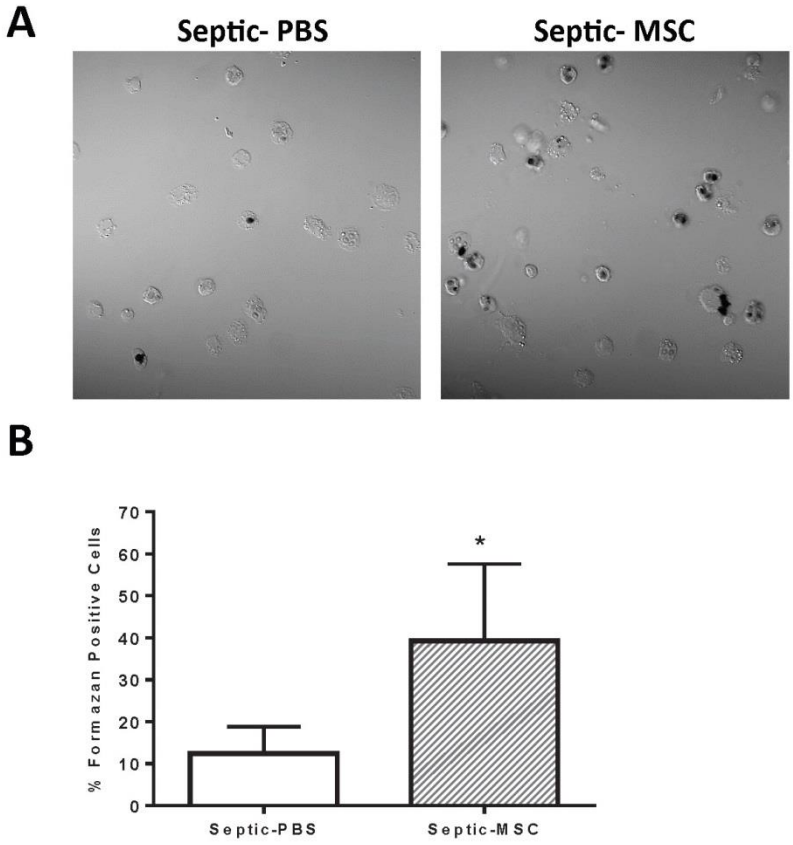
A
Septic- PBS
Septic- MSC
B
% Formazan Positive Cells
70
60
50
40
30
20
10
0
*
Septic-PBS
Septic-MSC

Figure 3

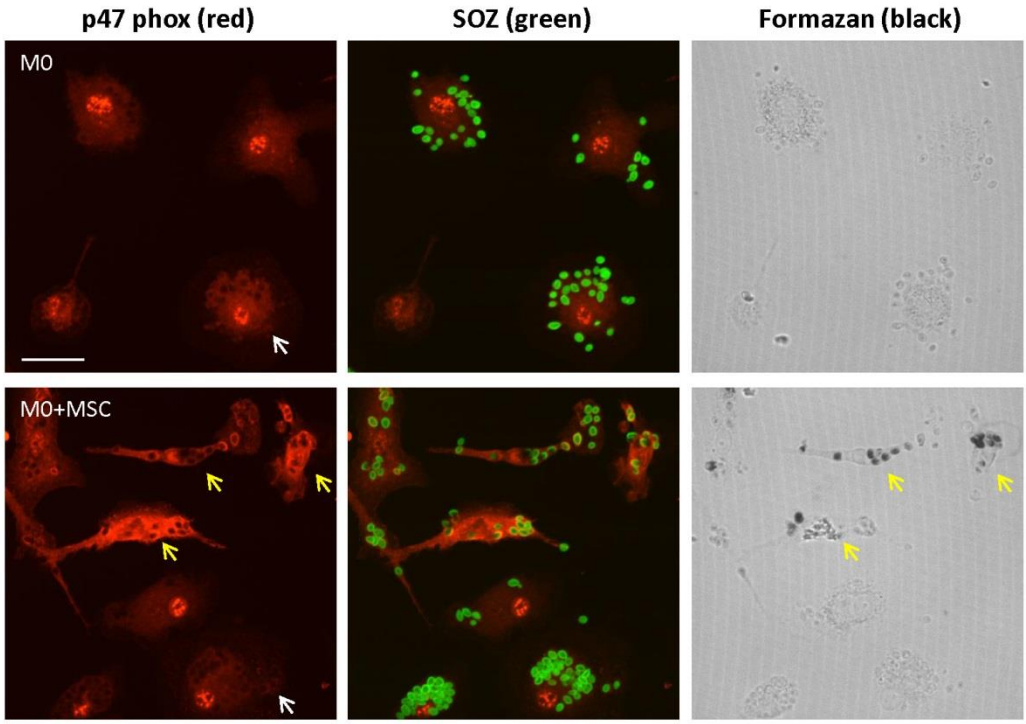

Figure 4

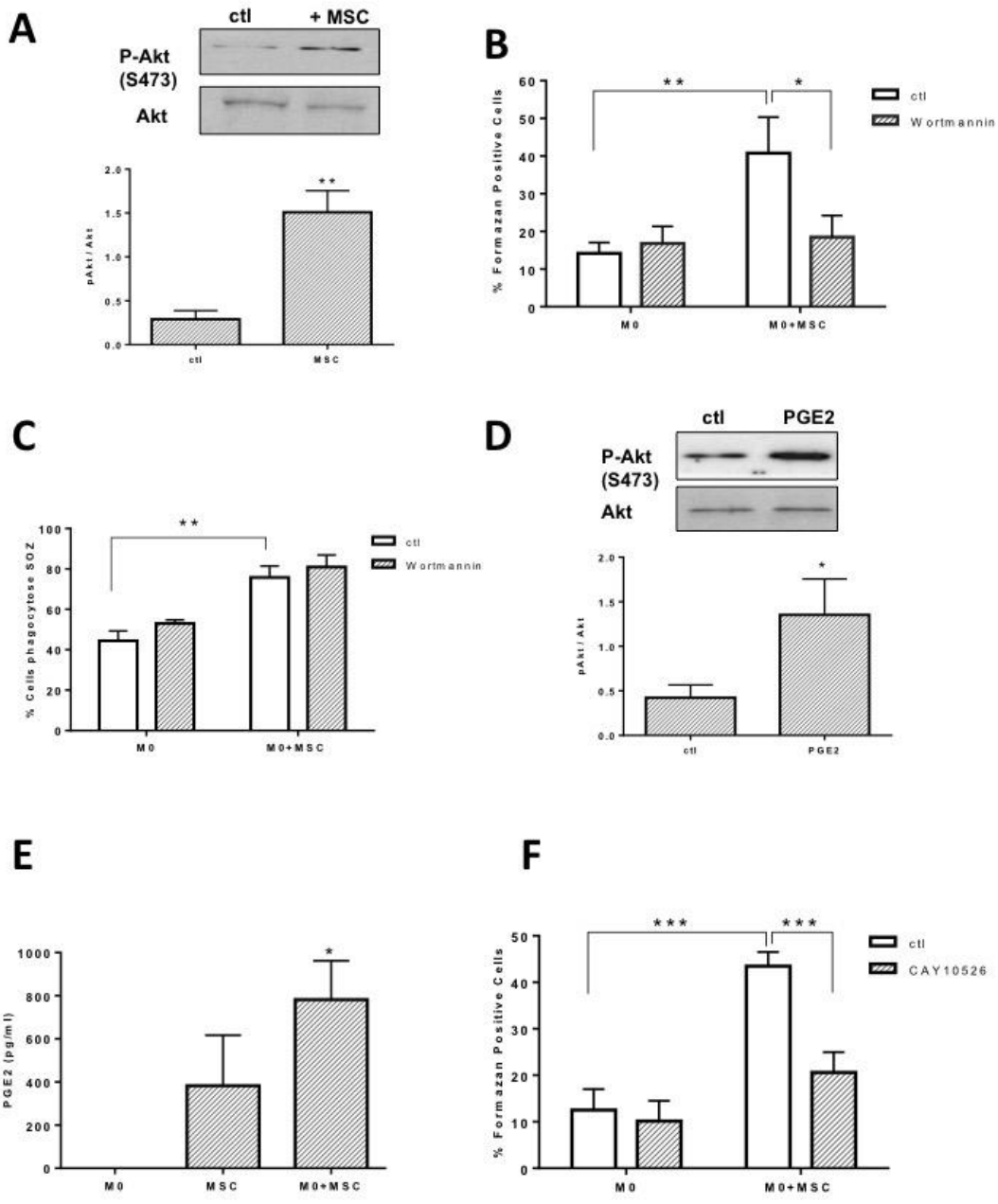
A
ctl
+ MSC
P-Akt
(S473)
Akt
pAkt / Akt
ctl
MSC
B
% Formazan Positive Cells
ctl
Wortmannin
M0
M0+MSC
C
% Cells phagocytose SOZ
ctl
Wortmannin
M0
M0+MSC
D
ctl
PGE2
P-Akt
(S473)
Akt
pAkt / Akt
ctl
PGE2
E
PGE2 (pg/ml)
M0
MSC
M0+MSC
F
% Formazan Positive Cells
ctl
CAY10526
M0
M0+MSC

Figure 5

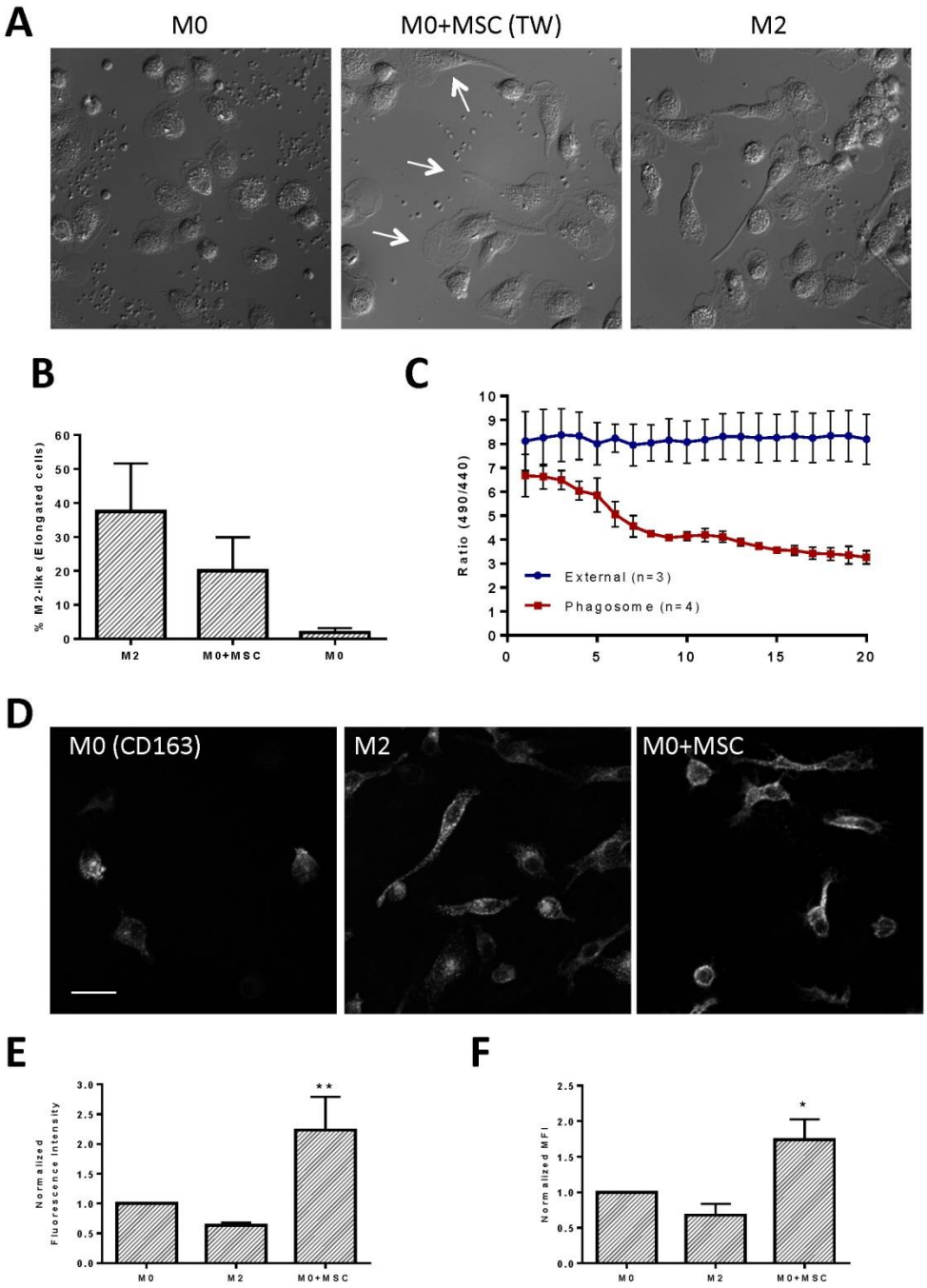
A
M0
M0+MSC (TW)
M2
B
% M2-like (Elongated cells)
M2
M0+MSC
M0
C
Ratio (490/440)
External (n=3)
Phagosome (n=4)
D
M0 (CD163)
M2
M0+MSC
E
Normalized Fluorescence Intensity
M0
M2
M0+MSC
F
Normalized MFI
M0
M2
M0+MSC

Figure 6

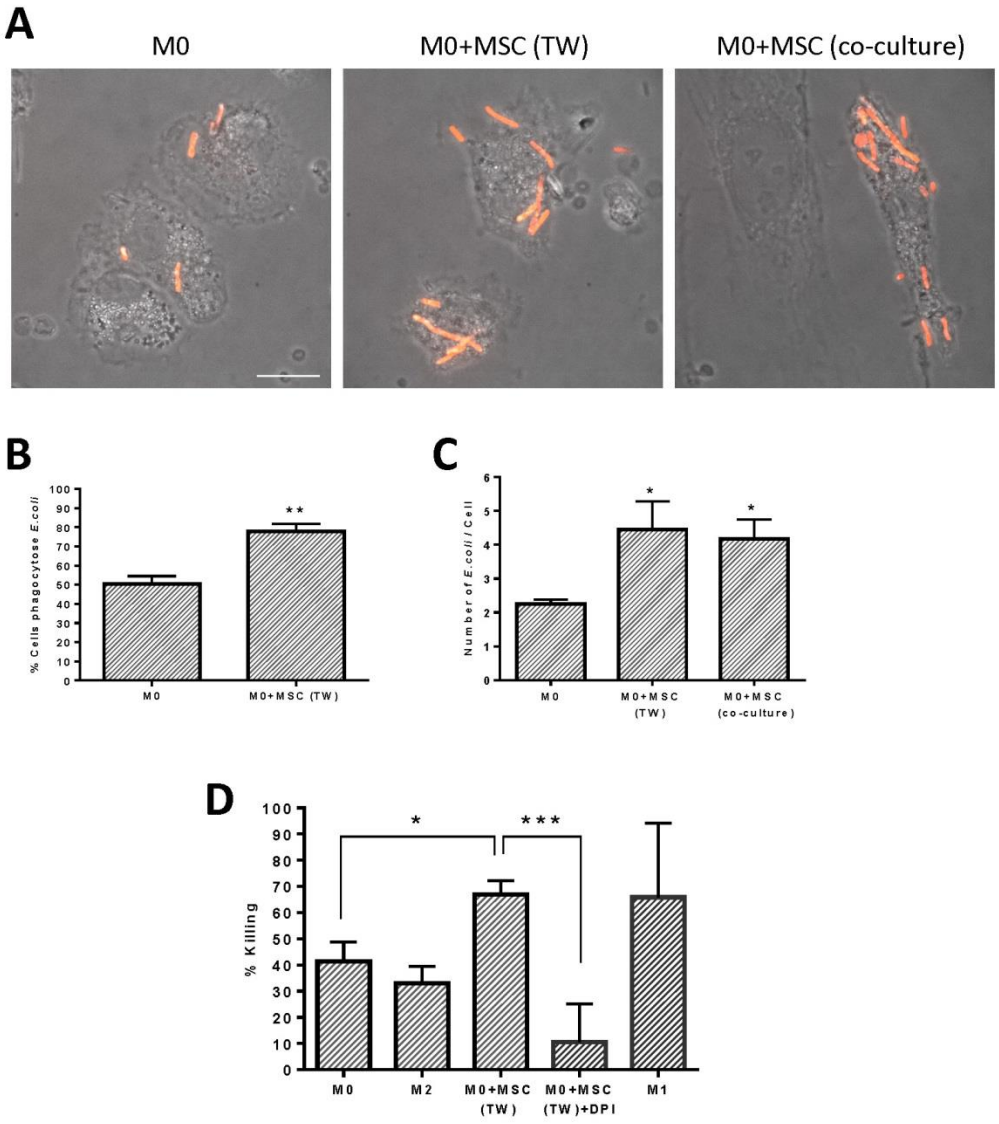
A
M0
M0+MSC (TW)
M0+MSC (co-culture)
B
% Cells phagocytose E.coli
M0
M0+MSC (TW)
C
Number of E.coli / Cell
M0
M0+MSC (TW)
M0+MSC (co-culture)
D
% Killing
M0
M2
M0+MSC (TW)
M0+MSC (TW)+DPI
M1

Figure 7

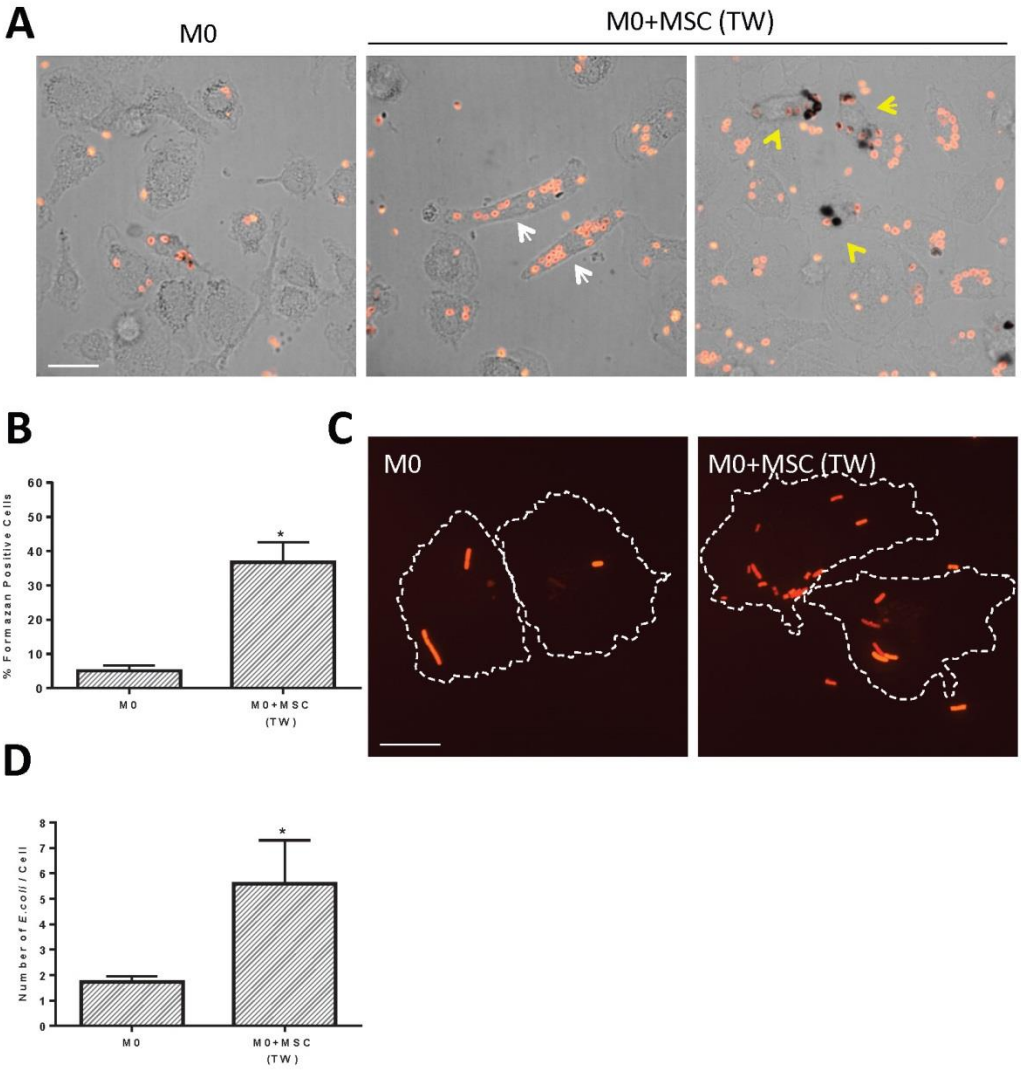
A
M0
M0+MSC (TW)
B
% Formazan Positive Cells
60
50
40
30
20
10
0
*
M0
M0+MSC (TW)
C
M0
M0+MSC (TW)
D
Number of E.coli / Cell
8
7
6
5
4
3
2
1
0
*
M0
M0+MSC (TW)

Figure 8

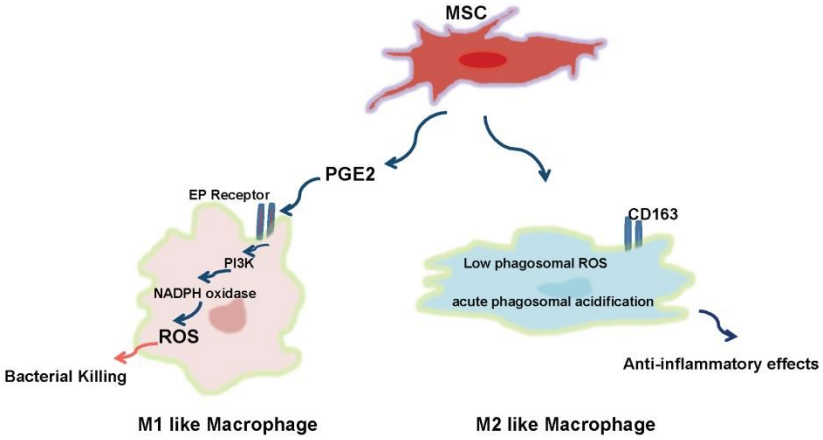
MSC
PGE2
EP Receptor
PI3K
NADPH oxidase
ROS
Bacterial Killing
CD163
Low phagosomal ROS
acute phagosomal acidification
Anti-inflammatory effects
M1 like Macrophage
M2 like Macrophage

Online Data Supplement

MATERIALS AND METHODS

MSC isolation and culture

Human bone marrow MSCs were obtained from the Center for the Preparation and Distribution of Adult Stem Cells (medicine.tamhsc.edu/irm/msc-distribution.html) at Texas A&M Health Science Center College of Medicine Institute for Regenerative Medicine (Temple, USA). The cells consistently differentiated into three lineages (bone, fat and chondrogenic cells) in culture, were negative for hematopoietic markers (CD34, CD36, CD117, and CD45) and positive for mesenchymal markers CD29 (95%), CD44 (>93%), CD49c (99%), CD49f (>70%), CD59 (>99%), CD90 (>99%), CD105 (>99%), and CD166 (>99%) [1]. The cells from the same donor, at passage 3 and 4, were used in all experiments. MSCs were cultured in MEM-α (Gibco, USA) media, supplemented with 10% Fetal Bovine Serum (FBS) (Gibco) and 1% antibiotics (streptomycin and penicillin) (Gibco), in 175 cm^2 flasks at 37°C in a humidified atmosphere containing 5% CO_2.

Animal experiments were carried out using umbilical cord MSCs. Human umbilical cords were obtained from full-term, consenting donors undergoing caesarean section at Mount Sinai Hospital, Toronto, Canada according to a protocol approved by research ethics boards at both the University of Toronto and Mount Sinai Hospital's Research Centre for Women's and Infants' Health (RCWIH). Human umbilical cord MSCs were non-enzymatically extracted by a proprietary methodology and provided by Tissue Regeneration Therapeutics (TRT) Inc., Toronto, Canada. Cells harvested by this process were cultured in Lonza TheraPEAK™ MSCGM-CD serum-free complete medium supplemented with antibiotics (28 µM Penicillin G, 104 µM Gentamycin, and 324 nM Amphotericin B) and culture-expanded on fibronectin-coated flasks for three passages prior to cryopreservation in 2 ml cryovials using a controlled rate freezer. Routine flow cytometry on identically processed lots revealed highly positive expression of CD90, CD73, CD105, CD140b and CD166 and lack of CD31, CD34, CD45 and MHC-II. On the day of administration, cells

were thawed in a 37^{o}C water bath and serially diluted in Lonza TheraPEAK basal medium prior to centrifugation and resuspension in PBS vehicle for delivery.

Human monocyte isolation, macrophage differentiation and culture

Human peripheral blood mononuclear cells (PBMCs) were isolated from the blood of healthy adult donors or patients with sepsis using dextran/Ficoll (Fig. 1, Fig. 3A-D, Fig. 5, Fig.6 & Fig. 7) or using Lympholyte cell separation media (Cedarlane Cat#CL5015) (Fig. 3E, and Fig. 4). Detailed protocols are provided in the Supplemental Materials. For defined macrophage polarization 25 ng/mL GM-CSF (for M1 macrophages) or 25 ng/mL M-CSF (for M2 macrophages) was added to the monocytes for 6 days. The macrophages were then treated for an additional 2 days with either LPS (500 ng/mL) plus IFN-γ (10 ng/mL) or IL-4 (15 ng/mL) for M1 and M2 macrophages, respectively, as reported previously [2-5].

Critically ill adult patients (age 18yrs and older) admitted to the intensive care unit within the previous 72 h meeting the criteria for sepsis [6] or with new onset of sepsis in the previous 72 h were enrolled into our study. Patients receiving corticosteroids, immunosuppressive agents, or blood transfusion or those infected with HIV were excluded. The study protocol was approved by the Research Ethics Board of St Michael's Hospital, and written informed consent was obtained from each subject or a surrogate.

Dermal fibroblasts culture

Normal Human Dermal Fibroblasts (NHDF) were purchased from Lonza (Mississauga, ON, Canada). The cells were seeded at a concentration of 6-7,000/cm^2 in 75 cm^2 tissue culture flask and maintained in FGM™-2 Fibroblast Growth Medium-2 supplemented with growth supplement kit (hFGF-B, Insulin, FBS, Gentamycin) from Lonza Canada.

Preparation of serum-opsonized zymosan

Dried Zymosan A (*S. cerevisiae*) Bioparticles (Life Technologies) were labeled with fluorophores (Alexa-555 or FITC) as reported previously [2]. Labeled zymosan was aliquoted and stored at −20°C. Prior to phagocytosis assays, fluorophore-conjugated zymosan was re-suspended in human serum at 2 mg/mL and incubated at 37°C for 60 min with constant agitation. The serum-opsonized zymosan was subsequently washed two times with PBS and used immediately.

Nitroblue tetrazolium (NBT) assay

NBT assays were performed as described previously [2]. Briefly, Alexa-555-conjugated SOZ and nitroblue tetrazolium (NBT, Sigma Cat#N5514-25TAB) were added to cells growing on 18-mm coverslips in 12-well plates at the concentrations indicated in the figure legends. The 12-well plate was then centrifuged for 1 min (1500 rpm) to rapidly bring the SOZ in contact with the cells. The cells were then incubated at 37˚C for 30 min. Excess particles were removed by three washes with PBS and the cells were fixed in 4% paraformaldehyde in PBS for 15 min. Cells were visualized by differential interference contrast microscopy on a Leica DM IRB microscope or by spinning disk confocal microscopy on a Zeiss Axiovert 200M microscope with a 63× objective and an additional 1.5× magnifying lens. The microscope is equipped with diode-pumped solid-state lasers (Spectral Applied Research) and a piezo focus drive. Images were acquired by a CCD camera (Hamamatsu Photonics) driven by Volocity software. Dark formazan deposits were indicative of phagosomal superoxide production. In some experiments after the NBT assay the cells were fixed in ice-cold methanol for 2 min at -20˚C and processed for immunofluorescence microscopy.

Luminol Assay

The luminol assay was adapted based on previous publications [2, 7]. Human monocyte-derived macrophages were prepared using the Lympholyte procedure and plated onto a 96 well white-sided plate (15K/well) and co-cultured or not with MSCs (5K) for 3 days. Prior to the assay, the cells were washed 1X with RPMI media without phenol red, then 100ul/ well of RPMI

media (without phenol red) containing 0.01 mg SOZ and 8U/ml HRP was added. The plate was centrifuged for 45 sec, then placed in an incubator for 4 min. The wells were washed 1X with 100 ul PBS and 100 ul of assay mixture was added (phenol red-free RPMI containing 8U/ml HRP, 50 U/ml SOD, 2000 U/ml catalase and 50 uM luminol). The plate was placed in a SpectraMax Luminometer (Molecular Devices, Inc) set to 37 C and luminescence was measured every 4 min.

Bacterial phagocytosis assay

Cultures of Red Fluorescent Protein (RFP)-expressing *E. coli (DH5a)* or RFP expressing *Burkholderia cenocepacia* were started from glycerol stocks and cultured overnight in 5 mL LB with the appropriate antibiotic added. The next day the cells were spun down in a microfuge (1 min max speed) then washed in PBS. The cells were re-suspended in 1 mL PBS and OD_{600} was measured to determine bacterial concentration. The bacteria were re-suspended in DMEM media without antibiotics. The bacteria were then added to macrophage cells grown on 18 mm glass coverslips in a 12-well plate at the concentration indicated in the figure legends. The plate was spun down (1500 rpm; 60 sec) then placed in a 37˚C incubator for 20 min. The cells were then washed 2X with PBS and fixed in 4% PFA/BSA for 15 min. For experiments with serum-opsonized bacteria, the bacteria were re-suspended in human serum and incubated for 1h at 37˚C with constant rotation, then washed once with PBS. Bacterial phagocytosis was monitored by spinning disk confocal microscopy.

Bacterial killing assay

Macrophage cells were cultured on 18 mm glass coverslips in 12 well plates in duplicate. The plates were washed 1X with PBS and unopsonized *E. coli* bacteria (~8.6 x 10^6 cells/mL) were re-suspended in serum-free DMEM media (without antibiotics) and added to the macrophage cells. For M1 cells the bacteria were opsonized with human serum for 1h, since M1 cells do not phagocytose unopsonized bacteria. The plates were spun down (1500 rpm; 60 sec) then placed in a 37˚C incubator for 20 min. The cells were then

washed 3X with warm PBS and DMEM media (with 5% FBS and 100 μg/mL gentamycin) was added for 25 min at 37˚C. The cells were then washed 3X with PBS. The cells in plate #1 were then lysed with 100 μL sterile 1%TX-100/PBS for 5 min, then 400 μL PBS was added and the lysates were plated onto LB plates. In plate #2 antibiotic-free DMEM media (with 5% FBS) was added and the plate was incubated for 1h at 37˚C. Plate #2 was then lysed and the lysate plated onto LB plates as described above. The next day bacterial colonies were counted and killing was expressed by dividing the number of colonies in plate #2 by the number in plate #1 and expressing as a percentage. In some experiments diphenyleneiodonium DPI (10 μM), a specific NADPH oxidase inhibitor [8], was added at the time of bacterial addition to the cells and was present throughout the experiment.

Immunofluorescence microscopy

Macrophage cells cultured on 18 mm glass coverslips were fixed in ice-cold methanol at -20˚C for 2 min. The cells were washed 3 times in PBS then incubated in 2%BSA/PBS for 1 h. Primary antibodies were then added overnight at 4˚C. The next day the cells were washed 3 times with PBS and Cy3 or Alexa488-conjugated rabbit anti-mouse secondary antibody was added for 1 h at room temperature. The cells were then washed with PBS and imaged by spinning disk confocal microscopy. Antibodies used: mouse monoclonal anti-CD163 (Clone 5C6-FAT, Novus Biologicals, Cat#BM4041); mouse monoclonal anti-NOX2 (gp91) (Clone 48, Abcam, Cat#ab139371); mouse monoclonal anti-human FcγRII (CD32) (Clone IV.3).

Phagosomal pH measurements

Phagosomal pH was measured as described previously [2]. Briefly, macrophage cells cultured on 18-mm coverslips were transferred to a Chamlide holder then incubated with FITC-conjugated SOZ (0.02 mg/mL). The holder was centrifuged for 30 sec (1500 rpm) to sediment the SOZ and then incubated for 2 min at 37˚C. The coverslip was washed gently 3 times with PBS and fresh media was added. The holder was then placed on a heated stage of a Leica DM IRB microscope and cells that had bound SOZ

were identified. SOZ particles were outlined using MetaFlour software and ratio imaging was performed every min for 20 min. Briefly, the cells were excited sequentially with 440 nm and 480 nm light and fluorescence emission at 550 nm was recorded as described previously [2, 9].

Flow cytometry

Macrophage cells were grown in 6-well plates and treated as outlined in the figure legends. The cells were then washed 2 times with PBS and 10 mM EDTA/ 0.1% BSA/ PBS was added and the cells were placed on ice for 20 min. The cells were then gently scraped, transferred to Eppendorf tubes and centrifuged at ~500 xg for 4 min. The supernatant was gently removed and 100 μL 2%BSA/PBS was added and the cells were re-suspended. Human Fc block solution (BD Pharmingen, Cat#564220) (1 μL) was added and samples were incubated on ice for 15 min. Fluorophore-labelled antibody was then added as per manufacturer's directions and incubated on ice for 30 min in the dark. The cells were then washed 3 times with 2%BSA/PBS, re-suspended in PBS and analyzed using a BD LSRFortessa X-20 cell analyzer. Unlabelled samples were used to gate negative vs. positive cell populations and propidium iodide added just prior to analysis was used to gate out dead or ruptured cells. Antibody used: FITC mouse anti-human CD163, Clone GHI/61 (BD Pharmingen, Cat#563697).

Statistical Analysis

All values reported are mean ±SD or ±SE as stated in the figure legends. An unpaired t-test assuming equal variance was used for two condition comparisons. ANOVA followed by Tukey's post-hoc test were used for multiple condition comparison. $p<0.05$ was considered significant.

References

1. Dominici M, Le Blanc K, Mueller I, Slaper-Cortenbach I, Marini F, Krause D, Deans R, Keating A, Prockop D, Horwitz E. Minimal criteria for defining multipotent mesenchymal stromal cells. The International Society for Cellular Therapy position statement. *Cytotherapy* 2006: 8(4): 315-317.
2. Canton J, Khezri R, Glogauer M, Grinstein S. Contrasting phagosome pH regulation and maturation in human M1 and M2 macrophages. *Mol Biol Cell* 2014: 25: 3330-3341.
3. Galli SJ, Borregaard N, Wynn TA. Phenotypic and functional plasticity of cells of innate immunity: macrophages, mast cells and neutrophils. *Nat Immunol* 2011: 12: 1035-1044.
4. Lawrence T, Natoli G. Transcriptional regulation of macrophage polarization: enabling diversity with identity. *Nat Rev Immunol* 2011: 11: 750-761.
5. Sica A, Mantovani A. Macrophage plasticity and polarization: in vivo veritas. *J Clin Invest* 2012: 122: 787-795.
6. Levy MM, Fink MP, Marshall JC, Abraham E, Angus D, Cook D, Cohen J, Opal SM, Vincent JL, Ramsay G, International Sepsis Definitions C. 2001 SCCM/ESICM/ACCP/ATS/SIS International Sepsis Definitions Conference. *Intensive Care Med* 2003: 29(4): 530-538.
7. Bylund J, Bjornsdottir H, Sundqvist M, Karlsson A, Dahlgren C. Measurement of respiratory burst products, released or retained, during activation of professional phagocytes. *Methods Mol Biol* 2014: 1124: 321-338.
8. Ellis JA, Mayer SJ, Jones OT. The effect of the NADPH oxidase inhibitor diphenyleneiodonium on aerobic and anaerobic microbicidal activities of human neutrophils. *Biochem J* 1988: 251(3): 887-891.
9. Demaurex N, Grinstein S. Measurement of endosomal pH in live cells by dual-excitation fluorescence imaging. *Cell Biology* 2006: Chapter 16: 163-169.

Supplemental data Figure Legends

Supplemental Fig. 1.

Effect of fibroblasts on phagosomal ROS production in human macrophages (NBT assay)

(**A**) Human blood-derived monocytes were cultured for 8 days with media containing serum (M0) or after 5 days the cells were cultured with fibroblasts in transwell (TW) or co-culture for 3 days. The cells were then incubated with 0.01 mg/ml serum-opsonized zymozan (SOZ) together with 0.125 mg/ml nitroblue tetrazolium (NBT). The cells were fixed and imaged by differential interference contrast microscopy. White arrows indicate cells with formazan deposits. Representative images shown for the various conditions.

Supplemental Fig. 2.

Some macrophage cells exposed to MSCs have low cell surface levels of the NADPH oxidase (NOX2) subunit gp91

Human blood-derived monocytes were cultured for 8 days with media containing serum (M0) or after 5 days the cells were cultured with bone barrow-derived MSCs in transwell (TW) or co-culture for 3 days. The cells were then immunostained for the NADPH oxidase (NOX2) subunit gp91. Both cell surface and intracellular expression was detected in control M0 cells and in round M0 cells in the M0+MSC condition (**A**, **B**, white arrows). In addition cells expressing low levels of gp91 (yellow arrows) were observed in the MO+MSC conditions both in transwell (**A**) and co-culture (**B**). Size bar;10 μm. (**C**) M0 cells co-cultured with MSCs were incubated with serum-opsonized Alexa555-conjugated zymozan together with 0.125 mg/ml NBT for 30 min. The cells were washed, fixed and immunostained for NADPH oxidase (gp91) (green). High gp91 levels were found in cells that were phagosomal formazan positive (white arrows) and relatively low levels in cells not producing phagosomal formazan (yellow arrow). (**D**) Total gp91 fluorescence intensity was quantified from cells in the various conditions. Only the round high expressing cells in the M0+MSC condition were used in the analysis. (**E**) Protein lysates were prepared from control M0 macrophages or M0 exposed

to MSCs in transwell. Immunoblot showing levels of gp91 (NOX2) and loading control protein actin.

Supplemental Fig. 3.

M1-like cells produced in response to MSC exposure do not express the M1 marker protein CD40

M1 macrophage cells were polarized as outlined in the Methods. Human blood-derived monocytes were cultured for 5 days then the cells were cultured with bone barrow-derived MSCs in transwell (TW) or co-cultured for 3 days. The cells were then incubated with serum-opsonized zymozan (SOZ) together with 0.125 mg/ml NBT for 30 min. The cells were fixed and immunostained for CD40. Extended focus, single confocal sections through the middle of the cells and light microscopy images are shown. CD40 was readily detected in most M1 cells with a primarily surface localization. Very low or no expression of CD40 was observed on MSC exposed macrophages, even in cells producing abundant phagosomal superoxide as detected by the NBT assay. Size bar; 10 μm.

Supplemental Fig. 4.

MSC exposure enhances human macrophage phagocytosis of unopsonized *Burkholderia cenocepacia*

Human blood-derived monocytes were cultured for 8 days with media containing serum (M0) or after 5 days the cells were cultured with bone barrow-derived MSCs or human skin fibroblasts in transwell (TW) or co-culture for 3 days. The cells were then incubated with live RFP-expressing *Burkholderia cenocepacia*, (~4x10^6 cells/ml) that were spun down onto the macrophage cells. Top left image shows extended focus image of combined phase contrast and RFP fluorescence of live M0 cells ~5 min after bacterial addition. For all other images shown, the cells were incubated with bacteria for 20 min at 37 C, washed with PBS, fixed, and imaged by light and fluorescence microscopy. Extended focus images of combined phase contrast and RFP fluorescence (63X magnification). Size bar; 10 μm.

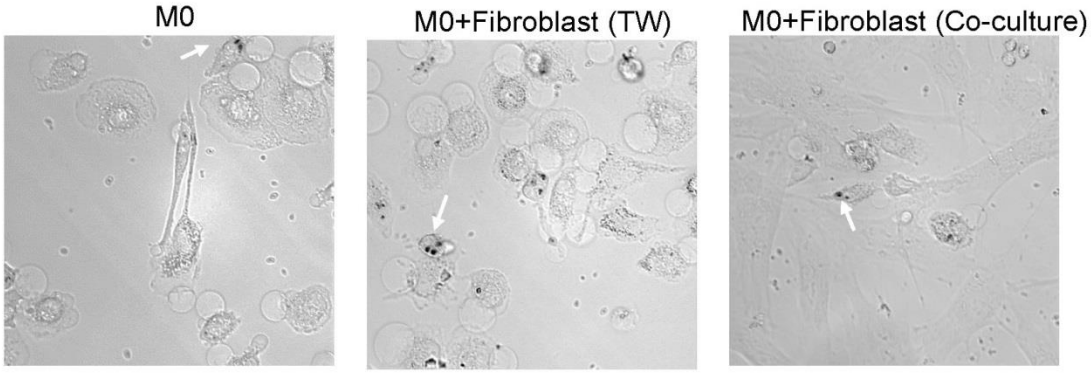
M0
M0+Fibroblast (TW)
M0+Fibroblast (Co-culture)

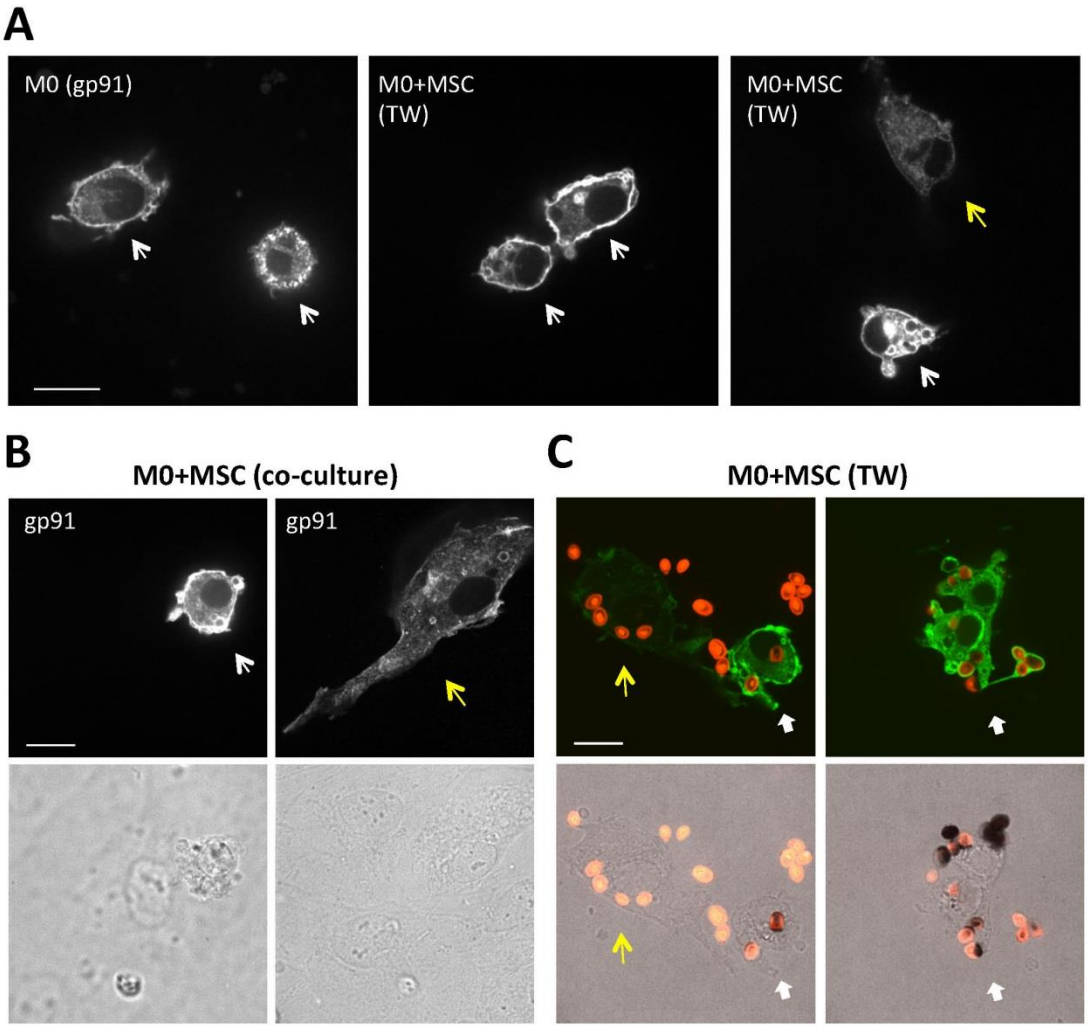
A
M0 (gp91)
M0+MSC
(TW)
M0+MSC
(TW)
B
M0+MSC (co-culture)
gp91
gp91
C
M0+MSC (TW)
gp91 (green); SOZ (red); Formazan (black)
D
gp91
(Normalized Fluorescence Intensity)
2.0
1.8
1.6
1.4
1.2
1.0
0.8
0.6
0.4
0.2
0.0
M0
M0+MSC
(TW)
M1
M2
E
M0
+
M0 MSC
125
93
72
gp91 (NOX2)
42
β-actin

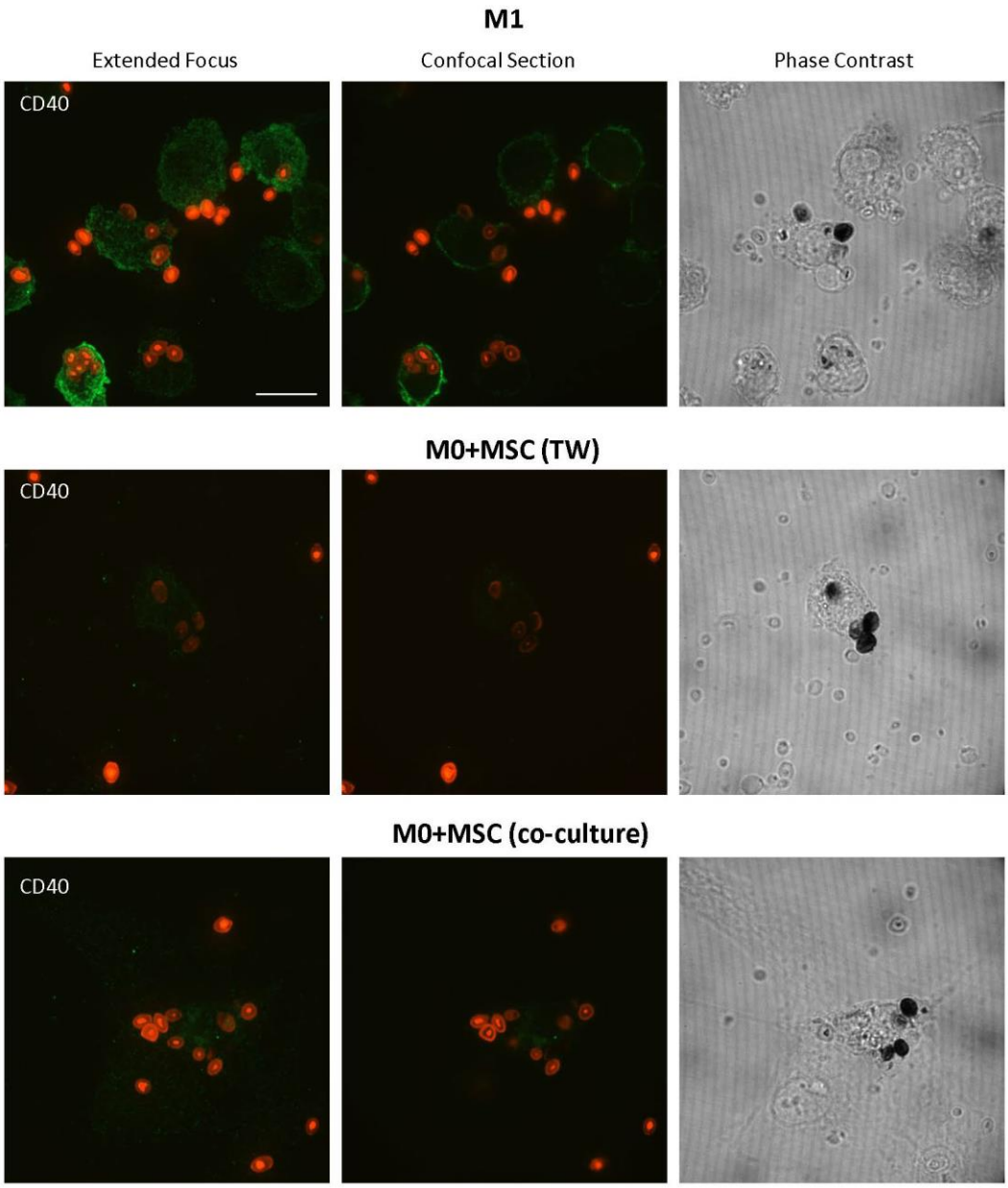
M1
Extended Focus
Confocal Section
Phase Contrast
CD40
M0+MSC (TW)
CD40
M0+MSC (co-culture)
CD40

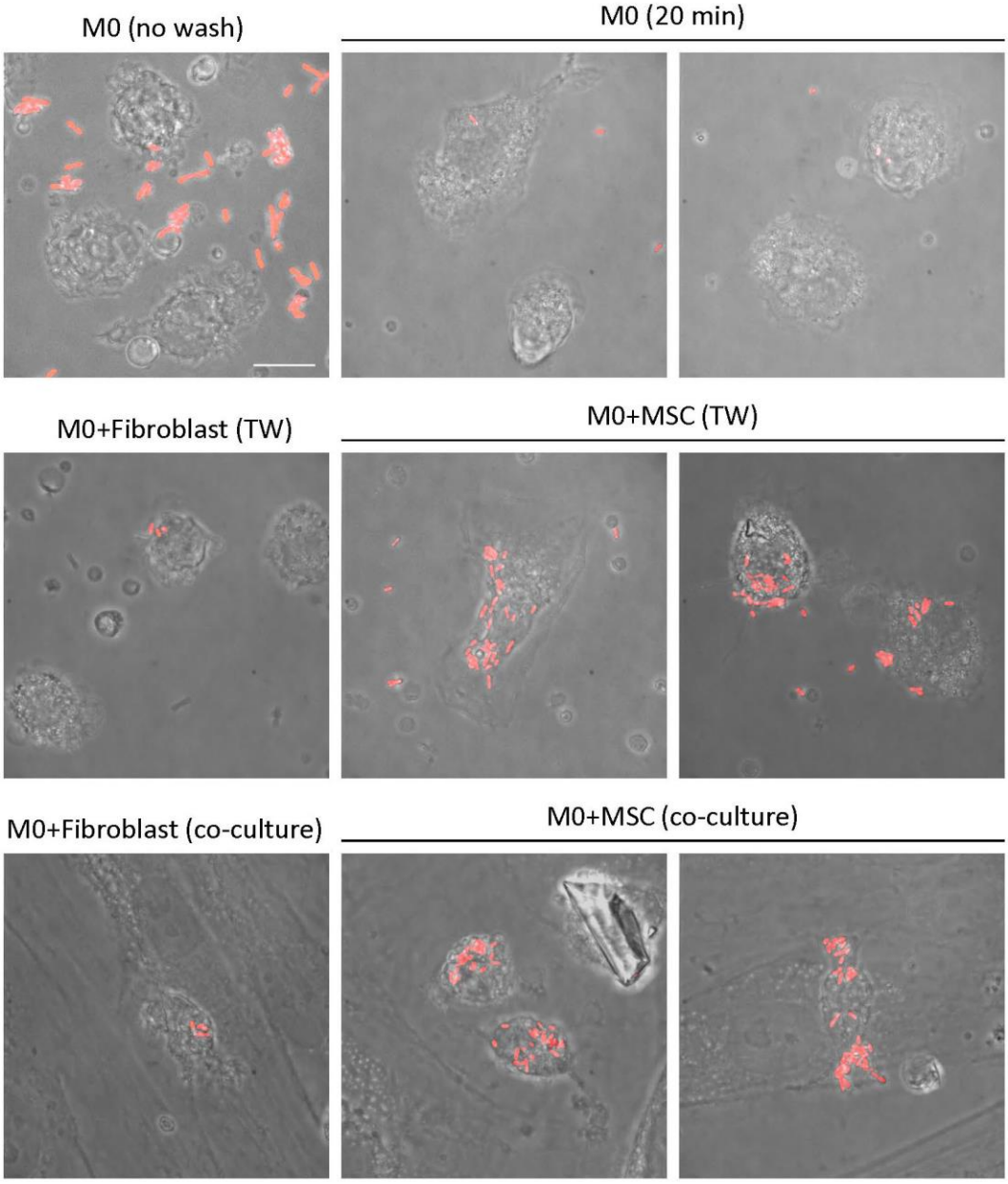
M0 (no wash)
M0 (20 min)
M0+Fibroblast (TW)
M0+MSC (TW)
M0+Fibroblast (co-culture)
M0+MSC (co-culture)